Rapid detection of DNA and RNA shrimp viruses using CRISPR-based diagnostics

Samuel R. Major[a], Matthew J. Harke[a], Roberto Cruz-Flores[b*], Arun K. Dhar[b], Andrea G. Bodnar[a], and Shelly A. Wanamaker[a#]

[a]Gloucester Marine Genomics Institute, Gloucester, MA, United States.

[b]Aquaculture Pathology Laboratory, School of Animal and Comparative Biomedical Sciences, The University of Arizona, Tucson, AZ, United States.

Running title: CRISPR diagnostics detect DNA and RNA shrimp viruses

[#]Please address manuscript correspondence to Shelly A. Wanamaker (shelly.wanamaker@gmgi.org).

[*]Present address: Centro de Investigación Científica y de Educación Superior de Ensenada, (CICESE), Carretera Ensenada-Tijuana No. 3918, Zona Playitas, 22860 Ensenada, Baja California, Mexico.

ABSTRACT

Timely detection of persistent and emerging pathogens is critical to controlling disease spread, particularly in high-density populations with increased contact between individuals and limited-to-no ability to quarantine. Standard molecular diagnostic tests for surveying pathogenic microbes have provided the sensitivity needed for early detection, but lag in time-to-result leading to delayed action. On-site diagnostics alleviate this lag, but current technologies are less sensitive and adaptable than lab-based molecular methods. Towards the development of improved on-site diagnostics, we demonstrated the adaptability of a loop-mediated isothermal amplification-CRISPR coupled technology for detecting DNA and RNA viruses that have greatly impacted shrimp populations worldwide; White Spot Syndrome Virus and Taura Syndrome Virus. Both CRISPR-based fluorescent assays we developed showed similar sensitivity and accuracy for viral detection and load quantification to real-time PCR. Additionally, both assays specifically targeted their respective virus with no false positives detected in animals infected with other common pathogens or in certified specific pathogen-free animals.

IMPORTANCE

The Pacific white shrimp (*Penaeus vannamei*) is one of the most valuable aquaculture species in the world but has suffered major economic losses from outbreaks of White Spot Syndrome Virus and Taura Syndrome Virus. Rapid detection of these viruses can improve aquaculture practices by enabling more timely action to be taken to combat disease outbreaks. Highly sensitive, specific, and robust CRISPR-based diagnostic assays such as those developed here have the potential to revolutionize disease management in agriculture and aquaculture helping to promote global food security.

40 **INTRODUCTION**

41 The ability to rapidly detect disease is a major challenge not just in human health but
42 across all farmed and wild animal health monitoring. While methods for disease detection have
43 advanced the field of molecular diagnostics to the global role it plays today, limitations posed by
44 laboratory-based technologies hinder the ability to quickly respond to disease outbreaks. For
45 example, culturing and molecular diagnostics using PCR-based methods provide the high
46 sensitivity needed for early pathogen detection, but they require laboratory processing (e.g.
47 sophisticated equipment, expensive reagents, and specialized training) leading to long turnaround
48 times for results (several days) and delayed action for disease mitigation (1–4). Contrastingly,
49 immunochromatographic antigen diagnostics are field-deployable, affordable and provide rapid
50 results, but comparatively lack sensitivity and require more time for assay creation resulting in a
51 longer time to respond to emerging pathogens (5). Alternative molecular diagnostics that require
52 less sophisticated equipment like loop-mediated isothermal amplification (LAMP) have recently
53 been developed, but their superior amplification efficiency can stochastically yield false positive
54 results (6). In human health, CRISPR-based molecular diagnostics, such as the SHERLOCK
55 (Specific High sensitivity Enzymatic Reporter UnLOCKing) technology, have emerged to
56 overcome the limitations of PCR and antigen tests to enable rapid, sensitive, inexpensive, and
57 accurate on-site detection of viruses and other pathogens (7). SHERLOCK combines the
58 efficiency of isothermal amplification with the specificity of CRISPR detection for highly
59 sensitive, specific, and robust diagnostics that can be used in low resource settings (8).
60 Applications beyond human health in veterinary pathology and disease diagnostics in agriculture
61 and aquaculture settings could have a tremendous impact on domestic and global food security.

The need for rapid, sensitive, and accurate diagnostics in aquaculture is imminent with production expected to double by 2050 to meet the demand of the growing population and being greatly impeded by infectious diseases (9, 10). For example, Pacific white shrimp (*Penaeus vannamei*) production, that accounts for ~25% of all seafood products consumed annually, has suffered major economic losses due to infections caused by viruses like White Spot Syndrome Virus (WSSV) and Taura Syndrome Virus (TSV) (11–13). These diseases have resulted in up to 100% mortality in as few as seven days (14, 15). The DNA virus WSSV has been the leading cause of economic losses in shrimp aquaculture globally since its emergence in 1991, costing ~$1 billion and reducing global shrimp production by ~10% annually (11). TSV, a single stranded RNA virus, has caused mass mortality events on at least five continents since its emergence in 1991, with an estimated total loss of $2 billion from 1992-1996 (16–18). Although Taura syndrome caused by TSV is no longer causing economic losses to the extent it has in the past, with the current availability and farming of TSV-tolerant shrimp lines (19), WSSV-tolerant shrimp are still under development and are not commercially available (20). The domestic development and international import of specific pathogen-free (SPF) shrimp stocks has mitigated some disease outbreaks. However, even with routine rigorous screening disease continues to be a major threat. For instance, shrimp stocks in Brazil and Colombia were reported to be contaminated from imported SPF shrimp with underlying TSV infection that went undetected (21). The more recently documented spread of WSSV in Australia, India, and Ecuador has resulted in the virus being labeled as the most devasting pathogen in the aquacultural history of shrimp farming (22–24). To ensure globally distributed stocks are disease-free and to mitigate production losses for improved food security, it is crucial that rapid, accurate, and sensitive diagnostics are available to shrimp farmers (25, 26).

85 To address the need for rapid diagnostics in shrimp aquaculture, SHERLOCK technology
86 has recently been applied to the detection of common and deadly shrimp viruses but remains to
87 be optimized. For example, a CRISPR-based diagnostic was developed to detect *Vibrio spp.* that
88 cause acute hepatopancreatic necrosis disease in shrimp but requires a two-step process of first
89 amplifying pathogen DNA with recombinase polymerase amplification (RPA) and then detecting
90 the amplicons with Cas12a in a separate reaction to detect down to 1000 copies per reaction (20
91 copies per µL in a 50 µL reaction) in 2 hours (27). Our lab developed a different variation of a
92 CRISPR-based diagnostic to detect WSSV in shrimp tissue that uses RPA to amplify WSSV
93 DNA, RNA polymerase to transcribe amplicons to RNA, and Cas13a to detect transcribed
94 amplicons (SHERLOCKv1) all in one tube (one-pot format) (28). This one-pot format reduces
95 time-to-result and was able to detect 10 viral copies per reaction in 60 minutes. Other reports
96 have found LAMP to be superior to RPA in speed and sensitivity (29, 30), and a second-
97 generation SHERLOCK assay that couples LAMP with a heat tolerant Cas enzyme, Cas12b,
98 showed highly sensitive, rapid, and robust detection of viral RNA from SARS-CoV-2 (31).
99 Building upon these successes, and incorporating second generation SHERLOCK technology,
100 we demonstrate the adaptability of this technology for both DNA and RNA viral targets and
101 present two second-generation SHERLOCK (SHERLOCKv2) assays that detect WSSV and
102 TSV. These robust, sensitive, and specific lab-based fluorescent assays can detect viral target in
103 shrimp tissue in 30 minutes without the need for thermocycling. They also enable field-
104 deployable conversion for improved diagnostic capabilities of viral outbreaks in aquaculture
105 settings. This demonstration of assay adaptation for diverse shrimp diseases paves the way for
106 next generation assay development in veterinary pathology and animal diagnostics for improved
107 disease management in aquaculture and agriculture.

RESULTS

Diagnostic assay development

Combining the robustness of LAMP with the specificity of CRISPR and detection of Cas12b collateral cleavage activity, we developed sensitive and specific one-pot SHERLOCKv2 assays for the detection of DNA and RNA viruses that negatively impact shrimp aquaculture worldwide, WSSV and TSV (**Figure 1**). In an initial screen to identify an optimal LAMP primer set targeting a conserved TSV genome region, we compared the amplification activity of three primer sets as well as a previously published LAMP primer set (32). We found the previously published set targeting the capsid protein gene between VP1 and VP3 domains showed the fastest, most sensitive detection of TSV and selected this set for the SHERLOCKv2 assay (**Figure 2a and c**). In designing the WSSV assay, the highly conserved viral protein 28 (VP28) was targeted to limit the ability of WSSV strain to influence detection. Of the four LAMP primer sets designed and screened, one set (VP28.31) showed superior speed (**Figure 2b and d**). The addition of poly-T linkers between the two annealing sites within the FIP and BIP primers increased both the speed and sensitivity of the primer set down to 100 copies (**Figure S1**). Of the 12 guide RNAs designed to target within the TSV LAMP target region (**Figure S2a**), one guide RNA (cr9225) produced cleavage signals before 30 minutes with low variance among replicate reactions and minimal background signal and was selected for the TSV SHERLOCKv2 assay (**Figure 3a**). Of the 11 guide RNAs designed to target within the WSSV LAMP target region (**Figure S2b**), one guide RNA (VP28_27) showed the highest cleavage signal with the greatest signal-to-background ratio and was selected for the WSSV SHERLOCKv2 assay (**Figure 3b**). Furthermore, we found that the addition of glycine, a reaction temperature of 62°C, 2 μM reporter concentration, and a guide RNA-to-Cas12b ratio of 1:1 consistently gave optimal signal-

131 to-background in the WSSV SHERLOCKv2 assay. Because the addition of carrier nucleic acid
132 has shown improvements to sensitivity and specificity in RT-LAMP reactions (33), we tested
133 this in the TSV SHERLOCKv2 assay and found that the addition of 5 or 10 ng of non-target
134 carrier RNA produced the highest signal with the least variance among replicates (**Figure S3**).
135 For WSSV SHERLOCKv2 assay, we decided to use 20 ng of non-target carrier DNA because
136 that was the upper limit of input material reported in the WSSV SHERLOCKv1 limit-of-
137 detection experiment and this amount would allow input for subsequent experiments to be
138 standardized. A step-by-step protocol for SHERLOCK assay development is provided in the
139 **Supplemental Material** along with a table of all oligos and DNA sequences used (**Table S1**)
140 and a table detailing all reaction components (**Table S2**).

141 *Assay sensitivity and specificity*

142 To evaluate assay sensitivity, we analyzed standard curves generated from 10-fold
143 dilutions of the synthetic TSV target RNA (8 independent experiments) and synthetic WSSV
144 target DNA (6 independent experiments), and both assays consistently detected down to 100
145 copies for WSSV (200 copies for TSV) with a strong correlation to the amount of nucleic acid
146 input (**Figure 4a-b and S4**). We found synthetic target to be comparable to genomic target
147 isolated from shrimp with high TSV and WSSV viral loads previously quantified by qPCR,
148 confirming that synthetic target can be used for estimating TSV and WSSV copy number
149 quantity in genomic samples (**Figure S4**). In experiments evaluating assay specificity, both
150 SHERLOCKv2 assays showed high specificity for their target pathogen. Only TSV-infected and
151 WSSV-infected shrimp samples showed Cas12b collateral cleavage signal compared to samples
152 from shrimp infected with other common shrimp pathogens (IMNV, IHHNV, EHP and *Vibrio*
153 *parahaemolyticus* causing AHPND/EMS) (**Figure 4c-d**). Furthermore, both assays showed no

false positive detection in samples from specific pathogen-free shrimp (**Figure 4c-d)**. While we did observe stochastic non-specific LAMP signal in some true negative samples, this did not lead to Cas cleavage and did not result in positive viral detection (**Figure S5**).

Assay validation

To estimate the diagnostic sensitivity of the SHERLOCKv2 assays, we tested shrimp samples from different TSV and WSSV challenge experiments in SHERLOCKv2 assays and in the OIE (World Organization for Animal Health) recommended real-time PCR diagnostic for TSV and WSSV (34). Assays were run alongside standard curves to quantify and compare viral copy number determined by each method (real-time PCR hereinafter referred to as qPCR). With regards to the TSV challenge experiments, there are lines of shrimp that show a continuum of susceptibility and resistance depending on the line's genetics and the TSV strain used to evaluate susceptibility (35). We therefore used two different genetic lines with two different isolates that represent two extremes of disease continuum. The Belize isolate used to infect the TSV-tolerant *P. vannamei* line is known to be highly virulent and has led to TSV infection in TSV-tolerant commercial *P. vannamei* lines, where the TSV-susceptible Kona line has shown high rates of infection regardless of the TSV isolate used in challenge experiments (36). Following viral challenge, the TSV-susceptible line displayed clinical manifestation of disease including pathognomonic lesions of TSV characterized by necrosis, pyknosis, and karyorrhexis of the cuticular epithelium within the appendages, gills, and exocuticle (**Figure 5a**). In addition, some of these showed mortalities during the course of the experiment. However, the TSV-tolerant *P. vannamei* showed no TSV-associated pathognomonic lesions or mortalities (**Figure 5b).** Because of the wide dynamic range in viral load expected in these samples, we did a titration experiment to determine an optimal amount of sample input for TSV detection with the TSV

SHERLOCK assay. We determined that 10 ng of TSV-infected shrimp genomic RNA led to the least variable and highest signal (**Figure S3**), and this amount was used for subsequent TSV SHERLOCKv2 and qPCR experiments. The qPCR detected TSV in all TSV-challenged shrimp samples (**Figures 5c**, **Table S3**). The TSV SHERLOCK assay detected TSV in 26 out of the 30 TSV-challenged shrimp samples (87% positive percent agreement) (**Table S3**). The four samples for which SHERLOCK did not detect TSV had low viral load extrapolated from a qPCR standard curve (three had < 1000 copies/µL and one had ~5000 copies/µL). Both qPCR or SHERLOCK TSV assays showed a significant effect of challenge experiment on the viral load (Mann-Whitney-U test $P = 0.006395$ and $P = 0.003415$, respectively), with the susceptible shrimp (Kona line) injected with the TSV El Salvador isolate generally showing a higher titer than the tolerant shrimp injected with the TSV Belize isolate. A Pearson's correlation analysis followed by a t-test showed a statistically significant correlation between viral copy concentration predicted by SHERLOCK that predicted by qPCR ($R = 0.93$, $p = 1.5\times10^{-11}$; **Figure 5d**) with SHERLOCK tending to underestimate viral copies relative to qPCR (**Figure 6a**).

For WSSV, we tested the same WSSV-infected *P. vannamei* samples previously quantified by the OIE-recommended WSSV qPCR and the SHERLOCKv1 assay (28). Given that these samples previously showed high viral loads and sample material was limited, 1 ng of WSSV-infected shrimp genomic DNA was used in each SHERLOCKv2 reaction. Of the 35 WSSV-infected *P. vannamei* samples tested alongside standard curves, we detected infection in 32 samples (91% positive percent agreement) (**Table S3**). The three samples where no WSSV was detected were expected to have low viral copies based on qPCR estimations (~40, 50, and 800 copies/µL). Moreover, viral copy concentrations measured by WSSV SHERLOCKv2 were

200 mostly similar to those quantified by qPCR (**Figure 6a**). Compared to the previous version
201 WSSV SHERLOCKv1 assay that used RPA and Cas13a enzymes (28), SHERLOCKv2 showed
202 less variation across technical replicates than SHERLOCKv1 (**Figure 6b**). A Pearson's
203 correlation analysis followed by a t-test showed a statistically significant correlation between
204 SHERLOCKv2 and qPCR viral copy quantifications (R = 0.79, $P = 9.8\times10^{-8}$), and between
205 SHERLOCKv2 and SHERLOCKv1 viral copy quantifications (R = 0.75, $P = 9.6\times10^{-7}$) (**Figure**
206 **7**).
207
208 **DISCUSSION**
209 With the goal of adapting cutting-edge human diagnostic technology to diseases
210 impacting food security, we developed two different rapid and highly specific lab-based one-pot
211 SHERLOCK fluorescent assays for the detection of common shrimp pathogens. We demonstrate
212 the adaptability of the SHERLOCK platform for targeting either a common RNA virus (TSV) or
213 a common DNA virus (WSSV) that have impacted shrimp aquaculture globally. We found the
214 TSV and WSSV SHERLOCKv2 assays to have a quantitative capability on par with the OIE-
215 recommended qPCR assays for these diseases. Moreover, both assays can assess infection status
216 for a variety of samples in as little as 30 minutes, improving upon the time-to-result of qPCR.
217 Without the need for thermocycling and with the demonstrated ease of converting a one-pot
218 fluorescent SHERLOCK assay to a field-deployable assay (8, 28), these assays lay the
219 foundation for rapid, specific field diagnostics in shrimp aquaculture.
220 Building on an earlier iteration of a WSSV SHERLOCK assay, we were able to simplify
221 assay components leading to more robust and repeatable detection of both DNA and RNA viral
222 targets. The previous WSSV SHERLOCK assay used RPA to amplify DNA target, RNA
223 polymerase to convert the amplified target from DNA to RNA, and Cas13a to detect RNA target

224 (28). The SHERLOCKv2 assays presented in this study use LAMP (with or without reverse
225 transcriptase) and Cas12b to detect DNA target from RNA or DNA input, following the
226 successful SARS-CoV-2 SHERLOCK assay design (31). By eliminating the need for converting
227 input material to RNA and relying on Cas13a for RNA detection, these SHERLOCKv2 assays
228 enable more stable and robust target detection. This is supported by the reduced variation across
229 technical replicates observed for WSSV SHERLOCKv2 compared to WSSV SHERLOCKv1.
230 Moreover, the use of LAMP in our assays makes them well-poised for use with a variety of
231 sample types including crude sample preparations. Although we did not test crude sample lysates
232 in this study, we have previously successfully demonstrated a paper matrix DNA extraction
233 method to be compatible with WSSV SHERLOCKv1. Given our past success and that the
234 LAMP enzyme (Bst 2.0 polymerase) is highly tolerant to inhibitors (37, 38), we foresee these
235 SHERLOCKv2 assays to be compatible with various sample types.

236 Pairing LAMP with CRISPR/Cas12b enabled these assays to overcome non-specific
237 signal that can occur in assays using LAMP alone. In the SHERLOCKv2 assays, stochastic non-
238 specific LAMP products did not lead to Cas cleavage signal. Although isothermal amplification-
239 based methods recently developed for aquaculture diagnostics have shown that sequence-specific
240 probes can enhance assay specificity (39, 40), the combination of primers and probes cannot
241 always be relied on for sequence-specific detection (41). Cas detection systems rely on sequence-
242 specific target binding to induce conformational change that triggers cleavage activity (42), and
243 combining isothermal amplification methods with this additional layer of specificity is becoming
244 more common in aquaculture molecular diagnostic approaches (28, 43). Despite reports of single
245 insertion and deletion tolerance in some Cas complexes (44), we found Cas12b to be highly

246 specific, supportive of previous reports of Cas12b specificity down to the single nucleotide level
247 (45).
248 Although disease diagnosis typically only requires a binary result, the ability to quantify
249 viral load can be useful. The significant correlations we found between SHERLOCKv2 assays
250 and qPCR assays suggest SHERLOCKv2 can be semi-quantitative. The TSV SHERLOCKv2
251 assay tended to underestimate viral copies relative to qPCR while the WSSV SHERLOCKv2
252 assay mostly showed similar viral copies to qPCR. These discrepancies could be explained by
253 differences in amplification efficiencies of different genomic target sequences. The TSV qPCR
254 assay targets near the beginning of the ORF1 (TSVgp1) region whereas the TSV SHERLOCK
255 assay targets near the end of the ORF2 region. The primers used for the OIE-recommended
256 WSSV qPCR protocol were designed to target a genomic region ~20 kb upstream of the VP28
257 gene region, while the LAMP primers and guide RNA for the WSSV SHERLOCK assay target
258 within the VP28 gene region itself. As amplification efficiency is affected by differences in
259 structure and sequence length in target regions as well as primers, it can be expected that
260 quantifications would differ between methods targeting different regions. Additionally, the
261 structural differences in the synthetic target standards used in the SHERLOCK assays (200-300
262 DNA or RNA fragments) and qPCR assays (plasmids) could have contributed to discrepancies in
263 results (46). Differences in data analysis between qPCR and SHERLOCKv2 methods could have
264 also contributed to discrepancies in viral detection among the infected shrimp samples. Samples
265 assessed in the qPCR assays were run in triplicate and considered to be positive if at least one
266 replicate had a Ct value ≤ 40 for diagnosis (34), while samples assessed in the SHERLOCKv2
267 assays were run in quintet and considered to be positive if at least three replicates passed a
268 baseline and an outlier threshold. The intention of this SHERLOCK scoring criteria was to

269 rigorously control for technical variation and precisely and confidently measure viral presence
270 and abundance in the development of these new assays. If the criteria were relaxed to require
271 only two samples passing the baseline threshold and not include an outlier threshold, TSV
272 infection would have been found in 29/30 samples (97% positive percent agreement) and WSSV
273 infection would have been found in 35/35 samples (100% positive percent agreement) (47). In
274 the future, the SHERLOCK scoring criteria used here can likely be relaxed following the testing
275 of larger number of samples. Similar to existing reports of the proportion of replicates testing
276 positive being relative to target concentration in both SHERLOCK and qPCR assays (48, 49), the
277 few samples with virus detected by qPCR and not by SHERLOCK were indeed closer to the
278 LODs of both TSV and WSSV assays. Despite the differences in analysis methods and in the
279 nature of template used to optimize the SHERLOCK assay compared to the qPCR assay, the
280 binary qualitative results in detecting virus in shrimp tissue showed positive percent agreements
281 (87% for TSV SHERLOCKv2 and 91% for WSSV SHERLOCKv2) and negative percent
282 agreements (100% for both assays) within or close to the strict range required by the FDA for
283 clinical SARS-CoV-2 assays (90% positive percent agreement and 95% negative percent
284 agreement) (50). Moreover, the quantitative loads of the corresponding viruses as measured by
285 the two assays were also comparable. This gives validity to the SHERLOCKv2 assays when
286 compared to the current gold standard of TSV and WSSV detection recommended by the OIE.
287 With molecular diagnostics rapidly advancing alongside outbreaks of existing and
288 emerging disease, the transfer of technology from human diagnostics to animal fields is critical,
289 particularly to those that support global food security. With a growing need to support
290 aquaculture production, we demonstrated the ability to adapt a SHERLOCK assay developed for
291 human diagnostics for detecting RNA and DNA shrimp pathogens. This development of novel (±

RT)-LAMP + CRISPR/Cas diagnostic assays for TSV and WSSV monitoring in *P. vannamei* and potential for field-deployable conversion will accelerate biomonitoring for shrimp aquaculture and pave the way for the developing rapid, efficient diagnostics across the agriculture field.

MATERIALS AND METHODS

Viral challenge experiments

For TSV, two independent challenge experiments were conducted using *P. vannamei* lines that differ in TSV susceptibility and TSV isolates that differ in virulence. The purpose of this was to generate tissues with a wide dynamic range of viral load. In one experiment, TSV-susceptible specific pathogen free (SPF) *P. vannamei* (Kona line) shrimp (N = 120) were injected with TSV inoculum (El Salvador isolate, Lightner et al. unpublished) intramuscularly and reared until animals were moribund (4 days). In a second experiment, individuals from a commercial line of TSV-tolerant SPF *P. vannamei* (N = 30) were injected with a TSV inoculum (Belize isolate (36)) intramuscularly. Shrimp were reared for 4-8 days in a single 1600 L tank containing 1000 L artificial sea water maintained at 27 ± 1 °C and a salinity of 30 ppt. No water change was done due to the short duration of the experiments. Shrimp tissues were processed for histopathology analysis following a standard procedure (51). Briefly, tissues were preserved in Davidson's AFA fixative for 48 hours after which the fixative was replaced with an equal volume of 70% ethanol. Samples were then washed in a series of alcohol/xylene solutions, embedded in paraffin, sectioned to 4µm using a microtome. The tissue sections were stained with hematoxylin and eosin, and examined using a bright field light microscope. Histopathological evaluations were performed using a subset of samples from the experimentally infected tolerant *P. vannamei* (N = 6) and susceptible *P. vannamei* (N = 5). The severity of the

315 TSV infection was graded based on a semi-quantitative scale ranging from Grade 0 to Grade 4:
316 Grade 0 showing no signs of infection; Grade 1 showing signs of infection by the pathogen but at
317 levels that may be below those needed for clinical disease classification; Grade 2 showing
318 moderate signs of infection based on the number and severity of pathogen-caused lesions; Grade
319 3 showing moderate to high signs of infection based on the number and severity of pathogen-
320 caused lesions; and Grade 4 showing high signs of infection based on a high number of
321 pathogen-caused lesions and tissue destruction (52). Total RNA from experimentally TSV-
322 challenged shrimp (N = 35) was extracted with the Total RNA Purification Kit (NORGEN
323 BIOTEK CORP) following the manufacturer's recommendations. Quality and quantity were
324 assessed using a NanoDrop™ (Thermo Fisher). The RNA concentrations of 30 samples were
325 normalized to approximately 15 ng μl^{-1} and TSV was detected and quantified from 2 µl of
326 sample using a TaqMan™ Fast Virus 1-Step Master Mix (Applied Biosystems™) following the
327 OIE recommended protocol and triplicate standards (mean $R^2 = 0.93 \pm 0.06$, mean efficiency
328 105.3% ± 15.28%) (53). All samples were run in triplicate alongside plasmid standards with
329 known copy numbers (100 - 1,000,000 copies). TSV load in the experimentally challenged
330 shrimp was calculated by extrapolating Ct values in the standard curve generated using plasmid
331 DNA template.
332 Unlike TSV, all commercially available *P. vannamei* lines are highly susceptible to
333 WSSV with shrimp mortality occurring 2-3 days post-challenge in routine bioassays conducted
334 in the Aquaculture Pathology Laboratory at University of Arizona. Details of the viral challenge
335 experiment with WSSV of *P. vannamei* are reported in Sullivan et al. 2019 (28). Briefly, specific
336 pathogen free shrimp (N = 137) were challenged by feeding WSSV (China isolate CN95 (54))
337 infected tissue and reared under the same conditions and duration as described above. Infection

338 was confirmed in moribund animals by histology as described above. Genomic DNA was
339 extracted with the DNeasy blood and tissue kit (Qiagen), quantified using a NanoDrop™
340 (Thermo Fisher), and quantified by qPCR using 1 µl of sample with TaqMan Fast Virus 1-Step
341 Master Mix run in triplicate on an ABI StepOne Plus system and following the OIE protocol
342 using triplicate standards (mean $R^2 = 0.99 \pm 0.0007$, mean efficiency 90.6 ± 12.0%) (55).

343 *TSV and WSSV SHERLOCK assay development*

344 To identify genomic targets for TSV and WSSV viral detection, publicly available viral
345 genome sequences were searched for consensus regions. For TSV, eight genomes were retrieved
346 from GenBank (https://www.ncbi.nlm.nih.gov/genbank/; JF966384.1 (56), NC_003005.1 (57),
347 JX094350.1 (58), AF277675.1(57), GQ502201.1 (59), DQ104696.1 (60), AY997025.1 (61),
348 DQ212790.1 (62)) and aligned with MAFFT (63) using the default parameters to generate a
349 consensus sequence (**Table S1**). For WSSV, the highly conserved viral envelope protein 28 (64)
350 was selected as a target and conservation across multiple strains was confirmed by surveying a
351 consensus genome compiled from 10 different isolates as previously reported (28).

352 To generate candidate LAMP primer sets, target sequences were input into the NEB
353 LAMP Primer Design tool (https://lamp.neb.com). For TSV, three LAMP primer sets were
354 selected as well as a previously published LAMP primer set (32) for screening. For WSSV, four
355 different candidate LAMP primer sets were selected and the primer set was optimized by testing
356 sets containing different combinations of primers as well as primer modifications including the
357 addition of a poly-T linker between the F1c/B1c and F2/B2 annealing sites of the FIP and BIP
358 primers (**Table S1**).

359 Guide RNAs for Cas12b collateral cleavage were designed using a sliding window of 20
360 bases in length and advancing one base at a time across the region between the F2 and B2

annealing sites of the LAMP FIP and BIP primers. To synthesize guide RNAs, a gBlock™ (IDT) containing the *Aap* Cas12b sgRNA scaffold sequence was first amplified using a forward primer containing the T7 promoter sequence and reverse primers containing each different spacer sequence. Amplification reaction conditions were as follows: 1X HF Buffer (NEB), 200 µM dNTPs (NEB), 0.5 µM forward primer, 0.5 µM reverse primer, 0.01 ng template DNA, and 1 unit Phusion DNA polymerase (NEB) in 50 µL. Reactions were run on a thermocycler (Applied Biosystems) with the following parameters: 98°C for 2 minutes, 30 cycles of 98°C for 10 seconds, 58°C for 30 seconds, and 72°C for 15 seconds, 72°C for 5 minutes, and a hold at 10°C. Products were gel purified using the QIAquick Gel Extraction kit (Qiagen) with a 2% agarose 1x TAE gel and products were eluted in 30 µL of Buffer EB prewarmed to 50°C. Concentrations were measured using the Qubit Broad Range dsDNA kit (Life Technologies). Next, *in vitro* transcription reactions were performed using the Ampliscribe T7 flash transcription kit (Lucigen) in a 40 µL reaction with 50 ng of DNA template, 9 mM of each ribonucleotide, 9 mM of DTT, 1 µL of RiboGuard RNase inhibitor, 4 µL of T7 RNA polymerase, and 1X transcription reaction buffer. Reactions were run at 42°C for 4 hours, incubated with 2 µL of DNase I (Lucigen) at 37°C for 15 minutes, and purified using the RNA Clean and Concentrate Kit (Zymo Research). Guide RNAs were quantified using the Qubit Broad Range RNA assay kit (Life Technologies) and molarity was estimated using the NEB copy number converter (https://nebiocalculator.neb.com/). All sequences from the consensus genome, gBlocks™ (IDT), primers, and guide RNAs are listed in **Table S1**.

Evaluating LAMP primers

For TSV, primer sets were screened against a synthetic TSV RNA target *in vitro* transcribed from gBlock™ DNA (IDT, **Table S1**) using the Ampliscribe T7-Flash Transcription

384 kit (Lucigen Corporation) and purified using the RNA Clean and Concentrator kit (Zymo
385 Research) following manufacturer's instructions. For WSSV, primer sets were screened against
386 either a synthetic WSSV DNA target (gBlock™, IDT; **Table S1**) or genomic DNA isolated from
387 shrimp with a high WSSV load. Target nucleic acid was diluted in background nucleic acid from
388 SPF shrimp as detailed in **Table S2e** to improve the specificity of the LAMP primers. Total
389 RNA from 10 SPF shrimp was isolated using the RNeasy blood and tissue kit (Qiagen) and
390 genomic DNA from 10 SPF shrimp was isolated using the DNeasy blood and tissue kit (Qiagen).
391 LAMP reactions were prepared as detailed in **Table S2a** and run at 60°C and 62°C (TSV and
392 WSSV; respectively) for 1 hour on a thermocycler for real-time PCR (QuantStudio 12K flex,
393 Thermo Fisher) with fluorescent measurements taken at 2-minute intervals. Successful primers
394 were determined by their ability to start amplification before 30 minutes.

395 *Evaluating guide RNAs and Cas12b detection*

396 Guide RNAs were systematically evaluated with Recombinant *Aap* Cas12b (GenScript)
397 for efficacy using TSV LAMP product or synthetic WSSV target DNA (gBlock™, IDT) in 20
398 µL (TSV) or 10 µL (WSSV) reactions described **Table S2b**. Prior to adding template and
399 reporter, reaction mixtures were incubated for 15 minutes at room temperature to facilitate the
400 formation of the CRISPR/Cas ribonucleoprotein complex. For each guide RNA, a negative
401 control was run that did not contain target nucleic acid to measure background collateral
402 cleavage, and all reactions were run in triplicate. Reactions were run in a 384-well black clear
403 bottom plate (Corning) at 60°C for 1 hour with measurements recorded every 2 minutes using a
404 Spectramax iD3 plate reader (Molecular Devices). Effective guide RNAs were identified as
405 those that generate a signal well-distinguished from the negative control in less than 30 minutes.

Evaluating sensitivity and standard curve generation

To produce standard curves for each assay, one-pot LAMP-Cas12b SHERLOCK reactions were run using either *in vitro* transcribed synthetic TSV RNA target, synthetic WSSV DNA target (gBlock™, IDT; **Table S1**), or genomic DNA isolated from shrimp with a high viral load. Ten-fold dilution series of synthetic DNA or RNA were made ranging from 10^1 to 10^6 copies μL^{-1} (TSV) or 10^1 to 10^{10} copies μL^{-1} (WSSV) with all samples diluted in specific pathogen free shrimp genomic RNA (5 ng per 20 µL reaction for TSV) or DNA (20 ng per 20 µL reaction for WSSV). Negative control reactions that did not contain any target nucleic acid were included in each experiment. Reactions were run with 5 replicates per sample prepared as detailed in **Table S2c** and run at 60°C (TSV) or 62°C (WSSV) using a QuantStudio 12k Flex thermocycler for real-time PCR (Applied Biosystems) for 60 minutes, with fluorescence readings every 2 minutes. Prior to adding dNTPs, *Bst* 2.0 DNA polymerase (New England BioLabs), primer mix, fluorescent reporter, SYTO-82 dye, or DNA, other reaction components were combined and incubated for 15 minutes at room temperature to facilitate the formation of the CRISPR/Cas ribonucleoprotein complex.

Evaluating SHERLOCK quantification

To compare quantification of viral loads estimated by the OIE-recommended qPCR and SHERLOCK, one-pot TSV SHERLOCK reactions were run on the same RNA samples from 30 TSV-infected shrimp quantified by qPCR described above. For WSSV, one-pot SHERLOCK reactions were run on the same DNA samples from 35 WSSV-infected shrimp previously quantified by qPCR (28). To standardize input across samples, 10 ng of RNA (TSV) or 1 ng of DNA (WSSV) was added per 20 µL SHERLOCK reaction. SHERLOCK reactions were prepared as detailed in **Table S2c**, and all samples were run alongside standard curves as

429 described above. A linear regression analysis was performed on Ct values from the standard
430 curve samples calculated from fluorescent measurements that were corrected to a baseline
431 defined by cycles 1-2 for WSSV and 1-4 for TSV, and viral copies were estimated for each
432 sample from the extrapolated standard Ct values. For each sample, including standards, any
433 replicate outlier based on a Ct value beyond the sample median Ct ± one cycle was excluded and
434 only samples with at least three out of five replicates were considered in downstream analyses.
435 Viral copies estimated by SHERLOCK one-pot reactions were then compared to those estimated
436 by qPCR using a Pearson correlation analysis followed by t-test with the stat_cor function in the
437 R package ggpubr (65).

438 *Evaluating specificity*

439 The specificity of each one-pot SHERLOCK assay was tested against either RNA or
440 DNA extracted from shrimp tissue infected with infectious myonecrosis virus (IMNV; muscle
441 tissue), infectious hypodermal and haematopoietic necrosis virus (IHHNV; muscle tissue), *V.*
442 *parahaemolyticus* causing acute hepatopancreatic necrosis disease/early mortality syndrome
443 (AHPND/EMS; hepatopancreas tissue), and *Enterocytozoon hepatopenaei* (EHP; hepatopancreas
444 tissue). RNA was extracted using RNeasy mini plus kit (Qiagen) and DNA was extracted using
445 the Qiagen DNeasy blood and tissue kit following manufacturer's protocols. One-pot reactions
446 were prepared as detailed in **Table S2c** with a total of 10 ng of sample RNA (TSV) or 1 ng of
447 sample DNA (WSSV) in each reaction. To estimate false positive rates, one-pot reactions were
448 prepared as detailed in **Table S2c** and run as described above with 5 ng of total RNA or 20 ng of
449 genomic DNA isolated from muscle tissue from 10 individual specific pathogen-free shrimp.

450 *Data availability*

Raw fluorescence data from all qPCR and SHERLOCK experiments, intermediate files, and R code used to generate plots and statistics are publicly available at https://doi.org/10.5281/zenodo.7438263 (47).

455 **ACKNOWLEDGEMENTS**

456 We thank Veronica L. Pereira and Zachary G. Dench (Gloucester Marine Genomics Institute) for
457 their contributions towards previous iterations of assay development that inspired the assay
458 design described here. We also thank New England BioLabs and Sherlock Biosciences for
459 helpful discussions and advice.

460

461 **FUNDING**

462 This work was supported by the United States Department of Agriculture NIFA AFRI
463 Exploratory Research Program (grant # 2018-08980)

464

465 **AUTHOR CONTRIBUTIONS**

466 S.R.M. and S.A.T. designed and performed molecular experiments, analyzed the data, and wrote
467 the manuscript; M.J.H provided input throughout the project and edited the manuscript; R.C.-F.
468 conducted histopathology and preliminary qPCR experiments; A.K.D. provided all laboratory
469 challenge samples, developed the experimental design, managed the histopathology verification,
470 provided input throughout the project, and contributed to manuscript revisions; A.G.B.
471 conceived the project, provided input throughout its progress, and edited the manuscript.

472

473 **REFERENCES**

474 1. Singh M, Bindal G, Misra CS, Rath D. 2022. The era of Cas12 and Cas13 CRISPR-based
475 disease diagnosis. https://doi.org/101080/1040841X20212025041 48:714–729.

476 2. Warke DrS. 2022. CRISPR-based tools: Alternative methods for diagnosis of diseases.
477 The Pharma Innovation Journal 11:1891–1896.

478 3. Cunha M V., Inácio J. 2014. Overview and challenges of molecular technologies in the
479 veterinary microbiology laboratory. Veterinary Infection Biology: Molecular Diagnostics
480 and High-Throughput Strategies 1247:3–17.

481 4. Esbin MN, Whitney ON, Chong S, Maurer A, Darzacq X, Tjian R. 2020. Overcoming the
482 bottleneck to widespread testing: A rapid review of nucleic acid testing approaches for
483 COVID-19 detection. RNA 26:771–783.

484 5. Jayamohan H, Lambert CJ, Sant HJ, Jafek A, Patel D, Feng H, Beeman M, Mahmood T,
485 Nze U, Gale BK. 2020. SARS-CoV-2 pandemic: a review of molecular diagnostic tools
486 including sample collection and commercial response with associated advantages and
487 limitations. Analytical and Bioanalytical Chemistry 2020 413:1 413:49–71.

488 6. Cammilleri G, Ferrantelli V, Pulvirenti A, Drago C, Stampone G, del Rocio Quintero
489 Macias G, Drago S, Arcoleo G, Costa A, Geraci F, di Bella C. 2020. Validation of a
490 Commercial Loop-Mediated Isothermal Amplification (LAMP) Assay for the Rapid
491 Detection of Anisakis spp. DNA in Processed Fish Products. Foods 9.

492 7. Gootenberg JS, Abudayyeh OO, Lee JW, Essletzbichler P, Dy AJ, Joung J, Verdine V,
493 Donghia N, Daringer NM, Freije CA, Myhrvold C, Bhattacharyya RP, Livny J, Regev A,
494 Koonin E V., Hung DT, Sabeti PC, Collins JJ, Zhang F. 2017. Nucleic acid detection with
495 CRISPR-Cas13a/C2c2. Science (1979) 356:438–442.

496 8. de Puig H, Lee RA, Najjar D, Tan X, Soekensen LR, Angenent-Mari NM, Donghia NM,
497 Weckman NE, Ory A, Ng CF, Nguyen PQ, Mao AS, Ferrante TC, Lansberry G, Sallum
498 H, Niemi J, Collins JJ. 2021. Minimally instrumented SHERLOCK (miSHERLOCK) for
499 CRISPR-based point-of-care diagnosis of SARS-CoV-2 and emerging variants. Sci Adv 7.

500 9. FAO. 2020. The State of World Fisheries and Aquaculture 2020. Sustainability in action.
501 1–244.

502 10. Naylor RL, Kishore A, Sumaila UR, Issifu I, Hunter BP, Belton B, Bush SR, Cao L,
503 Gelcich S, Gephart JA, Golden CD, Jonell M, Koehn JZ, Little DC, Thilsted SH,
504 Tigchelaar M, Crona B. 2021. Blue food demand across geographic and temporal scales.
505 Nat Commun 12:1–14.

506 11. Stentiford GD, Neil DM, Peeler EJ, Shields JD, Small HJ, Flegel TW, Vlak JM, Jones B,
507 Morado F, Moss S, others. 2012. Disease will limit future food supply from the global
508 crustacean fishery and aquaculture sectors. J Invertebr Pathol 110:141–157.

509 12. National Marine Fisheries Service. 2022. Fisheries of the United States, 2020. US
510 Department of Commerce, NOAA Current Fishery Statistics No. 2020.

13. Lafferty KD, Harvell CD, Conrad JM, Friedman CS, Kent ML, Kuris AM, Powell EN, Rondeau D, Saksida SM. 2015. Infectious diseases affect marine fisheries and aquaculture economics. Ann Rev Mar Sci 7:471–496.

14. Hasson KW, Lightner D V, Mohney LL, Redman RM, Poulos BT, White BM. 1999. Taura syndrome virus (TSV) lesion development and the disease cycle in the Pacific white shrimp *Penaeus vannamei*. Dis Aquat Organ 36:81–93.

15. Zhan W-B, Wang Y-H, Fryer JL, Yu K-K, Fukuda H, Meng Q-X. 1998. White spot syndrome virus infection of cultured shrimp in China. J Aquat Anim Health 10:405–410.

16. Brock JA. 1997. Taura syndrome, a disease important to shrimp farms in the Americas. World J Microbiol Biotechnol 13:415–418.

17. Lightner D v., Redman RM, Pantoja CR, Tang KFJ, Noble BL, Schofield P, Mohney LL, Nunan LM, Navarro SA. 2012. Historic emergence, impact and current status of shrimp pathogens in the Americas. J Invertebr Pathol 110:174–183.

18. Tu C, Huang H-T, Chuang S-H, Hsu J-P, Kuo S-T, Li N-J, Hsu T-L, Li M-C, Lin S-Y. 1999. Taura syndrome in Pacific white shrimp *Penaeus vannamei* cultured in Taiwan. Dis Aquat Organ 38:159–161.

19. Argue BJ, Arce SM, Lotz JM, Moss SM. 2002. Selective breeding of Pacific white shrimp (*Litopenaeus vannamei*) for growth and resistance to Taura Syndrome Virus. Aquaculture 204:447–460.

20. Lillehammer M, Bangera R, Salazar M, Vela S, Erazo EC, Suarez A, Cock J, Rye M, Robinson NA. 2020. Genomic selection for white spot syndrome virus resistance in whiteleg shrimp boosts survival under an experimental challenge test. Sci Rep 10.

21. Eswaran S. 2021. Specific Pathogen Free (SPF) Shrimps in Aquaculture, p. 465–470. *In* Pandey, P, Parhi, J (eds.), Advances in Fisheries Biotechnology. Springer, Singapore.

22. Sivakumar S, Vimal S, Abdul Majeed S, Santhosh Kumar S, Taju G, Madan N, Rajkumar T, Thamizhvanan S, Shamsudheen K v., Scaria V, Sivasubbu S, Sahul Hameed AS. 2018. A new strain of white spot syndrome virus affecting *Litopenaeus vannamei* in Indian shrimp farms. J Fish Dis 41:1129–1146.

23. Restrepo L, Reyes A, Bajaña L, Betancourt I, Bayot B. 2018. Draft genome sequence of a White Spot Syndrome Virus isolate obtained in Ecuador. Genome Announc 6.

24. Oakey HJ, Smith CS. 2018. Complete genome sequence of a white spot syndrome virus associated with a disease incursion in Australia. Aquaculture 484:152–159.

25. Jacobson RH, Wright P. 2022. Principles and methods of validation of diagnostic assays for infectious diseases, p. 11–26. *In* Manual of Diagnostic Tests for Aquatic Animals. World Organization of Animal Health (Office International des Epizooties).

26. Flegel TW. 2019. A future vision for disease control in shrimp aquaculture. J World Aquac Soc 50:249–266.

27. Li C, Lin N, Feng Z, Lin M, Guan B, Chen K, Liang W, Wang Q, Li M, You Y, Chen Q. 2022. CRISPR/Cas12a Based Rapid Molecular Detection of Acute Hepatopancreatic Necrosis Disease in Shrimp. Front Vet Sci 8:1693.

28. Sullivan TJ, Dhar AK, Cruz-Flores R, Bodnar AG. 2019. Rapid, CRISPR-based, field-deployable detection of White Spot Syndrome Virus in shrimp. Sci Rep 9:1–7.

29. Howson ELA, Kurosaki Y, Yasuda J, Takahashi M, Goto H, Gray AR, Mioulet V, King DP, Fowler VL. 2017. Defining the relative performance of isothermal assays that can be used for rapid and sensitive detection of foot-and-mouth disease virus. J Virol Methods 249:102.

30. Zou Y, Mason MG, Botella JR. 2020. Evaluation and improvement of isothermal amplification methods for point-of-need plant disease diagnostics. PLoS One 15:e0235216.

31. Joung J, Ladha A, Saito M, Kim N-G, Woolley AE, Segel M, Barretto RPJ, Ranu A, Macrae RK, Faure G, Ioannidi EI, Krajeski RN, Bruneau R, Huang M-LW, Yu XG, Li JZ, Walker BD, Hung DT, Greninger AL, Jerome KR, Gootenberg JS, Abudayyeh OO, Zhang F. 2020. Detection of SARS-CoV-2 with SHERLOCK one-pot testing. N Engl J Med 383:1492–1494.

32. Kiatpathomchai W, Jareonram W, Jitrapakdee S, Flegel TW. 2007. Rapid and sensitive detection of Taura syndrome virus by reverse transcription loop-mediated isothermal amplification. J Virol Methods 146:125–128.

33. Wei S, Suryawanshi H, Djandji A, Kohl E, Morgan S, Hod EA, Whittier S, Roth K, Yeh R, Alejaldre JC, Fleck E, Ferrara S, Hercz D, Andrews D, Lee L, Hendershot KA, Goldstein J, Suh Y, Mansukhani M, Williams Z. 2021. Field-deployable, rapid diagnostic testing of saliva for SARS-CoV-2. Sci Rep 11:1–9.

34. Tang-Nelson F-J, Lo C-F. 2021. Manual of Diagnostic Tests for Aquatic Animals 2021, 8th ed. World Organization of Animal Health (Office International des Epizooties). Retrieved 22 June 2022.

35. Moss SM, Doyle RW, Lightner D V. 2005. Breeding Shrimp for Disease Resistance: Challenges and Opportunities for Improvement. Diseases in Asian Aquaculture V 379–393.

36. Srisuvan T, Noble BL, Schofield PJ, Lightner D V. 2006. Comparison of four Taura syndrome virus (TSV) isolates in oral challenge studies with *Litopenaeus vannamei* unselected or selected for resistance to TSV. Dis Aquat Organ 71:1–10.

37. Kaneko H, Kawana T, Fukushima E, Suzutani T. 2007. Tolerance of loop-mediated isothermal amplification to a culture medium and biological substances. J Biochem Biophys Methods 70:499–501.

38. Tanner N. 2015. Improved reagents for Isothermal DNA amplification. New England Biolabs 1–3.

39. Zhang T, Liu X, Yang X, Liu F, Yang H, Li X, Feng H, Wu X, Jiang G, Shen H, Dong J. 2022. Rapid on-site detection method for White Spot Syndrome Virus using Recombinase

Polymerase Amplification combined with lateral flow test strip technology. Front Cell Infect Microbiol 12:1008.

40. Kampeera J, Dangtip S, Suvannakad R, Khumwan P, Senapin S, Kiatpathomchai W. 2021. Reverse transcription loop-mediated isothermal amplification (RT-LAMP) combined with colorimetric gold nanoparticle (AuNP) probe assay for visual detection of tilapia lake virus (TiLV) in Nile and red hybrid tilapia. J Fish Dis 44.

41. Hardinge P, Murray JAH. 2019. Lack of specificity associated with using molecular beacons in loop mediated amplification assays. BMC Biotechnol 19.

42. Saha A, Arantes PR, Hsu R v., Narkhede YB, Jinek M, Palermo G. 2020. Molecular dynamics reveals a DNA-induced dynamic switch triggering activation of CRISPR-Cas12a. J Chem Inf Model 60.

43. Naranitus P, Aiamsa-at P, Sukonta T, Hannanta-anan P, Chaijarasphong T. 2022. Smartphone-compatible, CRISPR-based platforms for sensitive detection of acute hepatopancreatic necrosis disease in shrimp. J Fish Dis 45:1805–1816.

44. Zhang W, Shi R, Dong K, Hu H, Shu W, Mu Y, Yan B, Li L, Xiao X, Wang H. 2022. The off-target effect of CRISPR-Cas12a system toward insertions and deletions between target DNA and crRNA sequences. Anal Chem 94:8596–8604.

45. Teng F, Guo L, Cui T, Wang XG, Xu K, Gao Q, Zhou Q, Li W. 2019. CDetection: CRISPR-Cas12b-based DNA detection with sub-attomolar sensitivity and single-base specificity. Genome Biol 20:132.

46. Bowers RM, Dhar AK. 2011. Effect of template on generating a standard curve for absolute quantification of an RNA virus by real-time reverse transcriptase-polymerase chain reaction. Mol Cell Probes 25:60–64.

47. Trigg SA. 2022. shellytrigg/paper-TSV_WSSV_SHERLOCKv2: TSV-WSSV-SHERLOCKv2_ms (v5.0). Zenodo. https://doi.org/10.5281/zenodo.7438263.

48. Cowley JA, Rao M, Coman GJ. 2018. Real-time PCR tests to specifically detect IHHNV lineages and an IHHNV EVE integrated in the genome of *Penaeus monodon*. Dis Aquat Organ 129.

49. Lee RA, De Puig H, Nguyen PQ, Angenent-Mari NM, Donghia NM, McGee JP, Dvorin JD, Klapperich CM, Pollock NR, Collins JJ. 2020. Ultrasensitive CRISPR-based diagnostic for field-applicable detection of *Plasmodium* species in symptomatic and asymptomatic malaria. Proc Natl Acad Sci U S A 117.

50. Brooks ZC, Das S. 2020. COVID-19 testing impact of prevalence, sensitivity, and specificity on patient risk and cost. Am J Clin Pathol 154:575–584.

51. Bell TA, Lightner DV. 1988. Handbook of normal penaeid shrimp histology. The World Aquaculture Society, Baton Rouge, LA.

52. Lightner DV (ed.). 1996. A handbook of shrimp pathology and diagnostic procedures for diseases of cultured penaeid shrimp. Baton Rouge, LA (USA) World Aquaculture Society.

53. Tang KFJ, Wang J, Lightner D V. 2004. Quantitation of Taura syndrome virus by real-time RT-PCR with a TaqMan assay. J Virol Methods 115:109–114.

54. Cruz-Flores R, Mai HN, Kanrar S, Aranguren Caro LF, Dhar AK. 2020. Genome reconstruction of white spot syndrome virus (WSSV) from archival Davidson's-fixed paraffin embedded shrimp (*Penaeus vannamei*) tissue. Sci Rep 10.

55. Durand S V., Lightner D V. 2002. Quantitative real time PCR for the measurement of white spot syndrome virus in shrimp. J Fish Dis 25:381–389.

56. Aranguren LF, Salazar M, Tang K, Caraballo X, Lightner D. 2013. Characterization of a new strain of Taura syndrome virus (TSV) from Colombian shrimp farms and the implication in the selection of TSV resistant lines. J Invertebr Pathol 112:68–73.

57. Mari J, Poulos BT, Lightner D V., Bonami JR. 2002. Shrimp Taura syndrome virus: Genomic characterization and similarity with members of the genus *Cricket* paralysis-like viruses. Journal of General Virology 83:915–926.

58. Tang KFJ, Navarro SA, Pantoja CR, Aranguren FL, Lightner D v. 2012. New genotypes of white spot syndrome virus (WSSV) and Taura syndrome virus (TSV) from the Kingdom of Saudi Arabia. Dis Aquat Organ 99:179–185.

59. Dhar AK, Lakshman DK, Amundsen K, Robles-Sikisaka R, Kaizer KN, Roy S, Hasson KW, Allnutt FCT. 2010. Characterization of a Taura syndrome virus isolate originating from the 2004 Texas epizootic in cultured shrimp. Arch Virol 155:315–327.

60. Huang XX, Lu CP. 2005. The molecular diagnosis and phylogenetic analysis of Taura Syndrome Virus isolated in China. https://www.ncbi.nlm.nih.gov/nuccore/DQ104696.1.

61. Srisuvan T, Tang KFJ, Lightner D v. 2005. Experimental infection of *Penaeus monodon* with Taura syndrome virus (TSV). Dis Aquat Organ 67:1–8.

62. Côté I, Navarro S, Tang KFJ, Noble B, Lightner D v. 2008. Taura syndrome virus from Venezuela is a new genetic variant. Aquaculture 284:62–67.

63. Katoh K, Misawa K, Kuma KI, Miyata T. 2002. MAFFT: a novel method for rapid multiple sequence alignment based on fast Fourier transform. Nucleic Acids Res 30:3059–3066.

64. You Z, Nadala ECB, Yang J, Loh PC. 2004. Conservation of the DNA sequences encoding the major structural viral proteins of WSSV. Dis Aquat Organ 61:159–163.

65. Alboukadel K. 2020. ggpubr: "ggplot2" Based Publication Ready Plots. R package version 0.4.0.

660

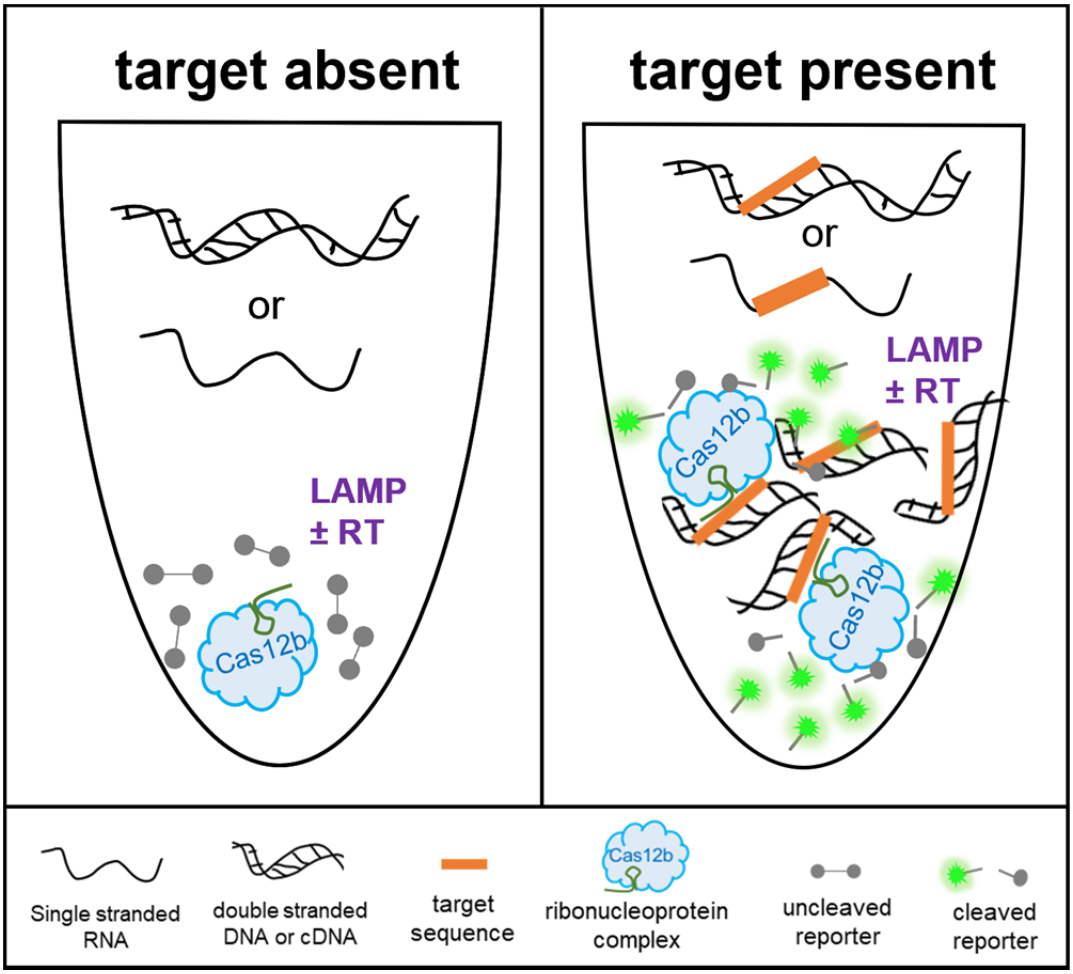

661

662 **Figure 1.** Schematic for CRISPR-based DNA and RNA detection in a one-pot reaction. When
663 the TSV or WSSV target sequence is absent, there is no amplification and no CRISPR-Cas
664 mediated cleavage of the reporter molecule. When the TSV or WSSV target sequence is present,
665 there is isothermal amplification of the target sequence and simultaneous detection by CRISPR-
666 Cas target binding and collateral cleavage of a fluorescent reporter. LAMP ± RT signifies the
667 need for reverse transcriptase (RT) and LAMP for the amplification of the TSV RNA target or
668 need for LAMP only for the amplification of the WSSV DNA target.

669

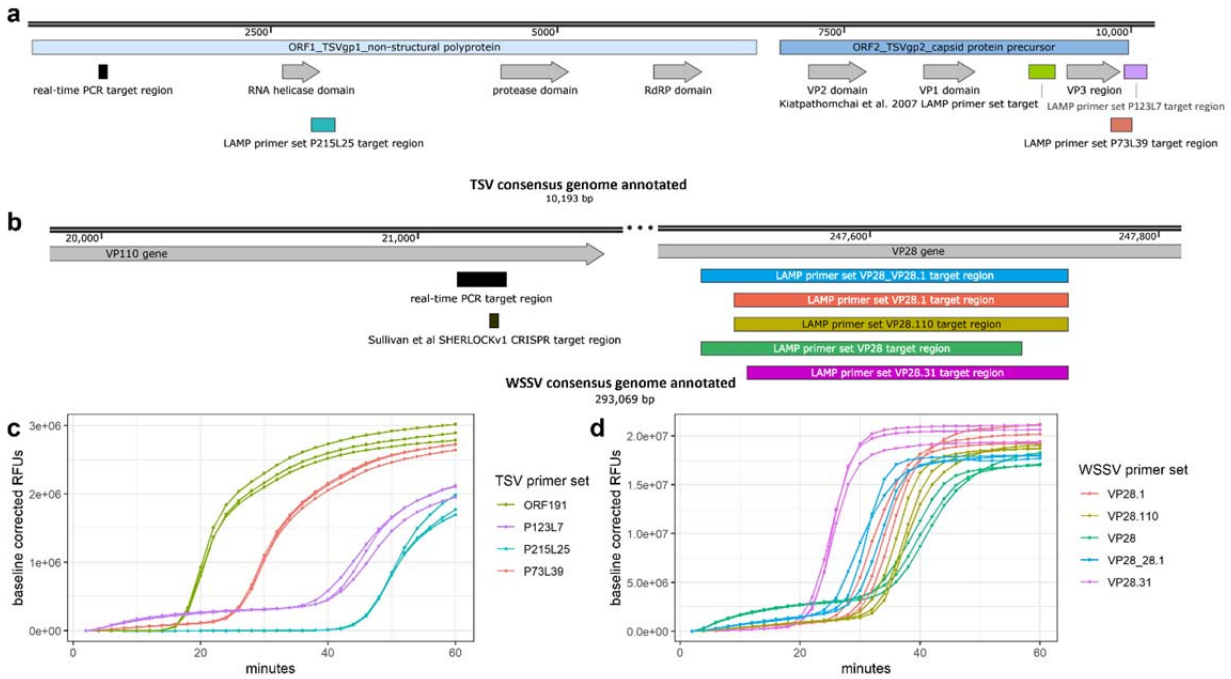

Figure 2. TSV and WSSV LAMP primer design and screening. (**a**) Annotated TSV consensus genome showing OIE standard diagnostic real-time PCR target region in black and LAMP target regions in teal, green, purple, and coral. (**b**) Annotated portions of WSSV consensus genome showing OIE standard diagnostic real-time PCR target region in black, the SHERLOCKv1 target region in brown, and LAMP target regions in blue, coral, gold, green, and magenta. (**c**) Amplification plot of triplicate LAMP reactions screening four different TSV primer sets (indicated by different colors) using 1,000,000 target copies of TSV. (**d**) Amplification plot of triplicate LAMP reactions screening five different WSSV primer sets (indicated by different colors) using 1,000,000 target copies of WSSV.

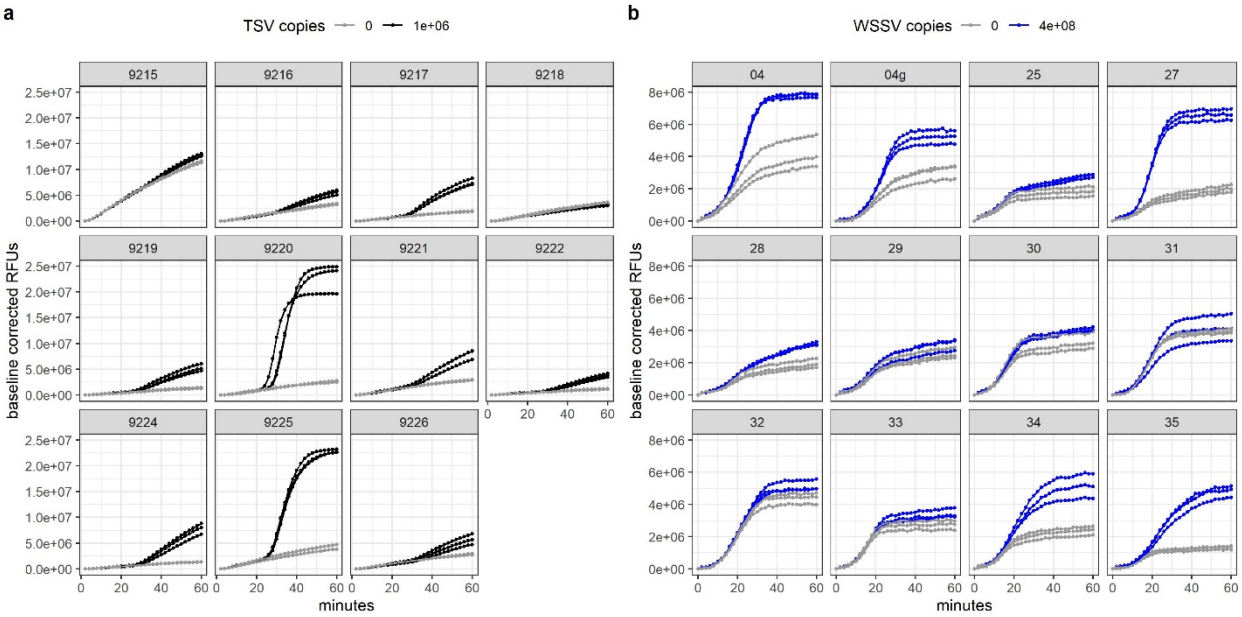

Figure 3. TSV and WSSV guide RNA screening. (**a**) Plots showing Cas12b collateral cleavage activity of each different TSV guide RNA when 1,000,000 (black) or 0 (gray) copies of TSV RNA target is present. (**b**) Plots showing Cas12b collateral cleavage activity of each different WSSV guide RNA when 400,000,000 (blue) or 0 (gray) copies of WSSV DNA target is present. '04g' is the same sequence as '04' but it was transcribed from a gBlock™ instead of an amplicon (see **Materials and Methods** for more details).

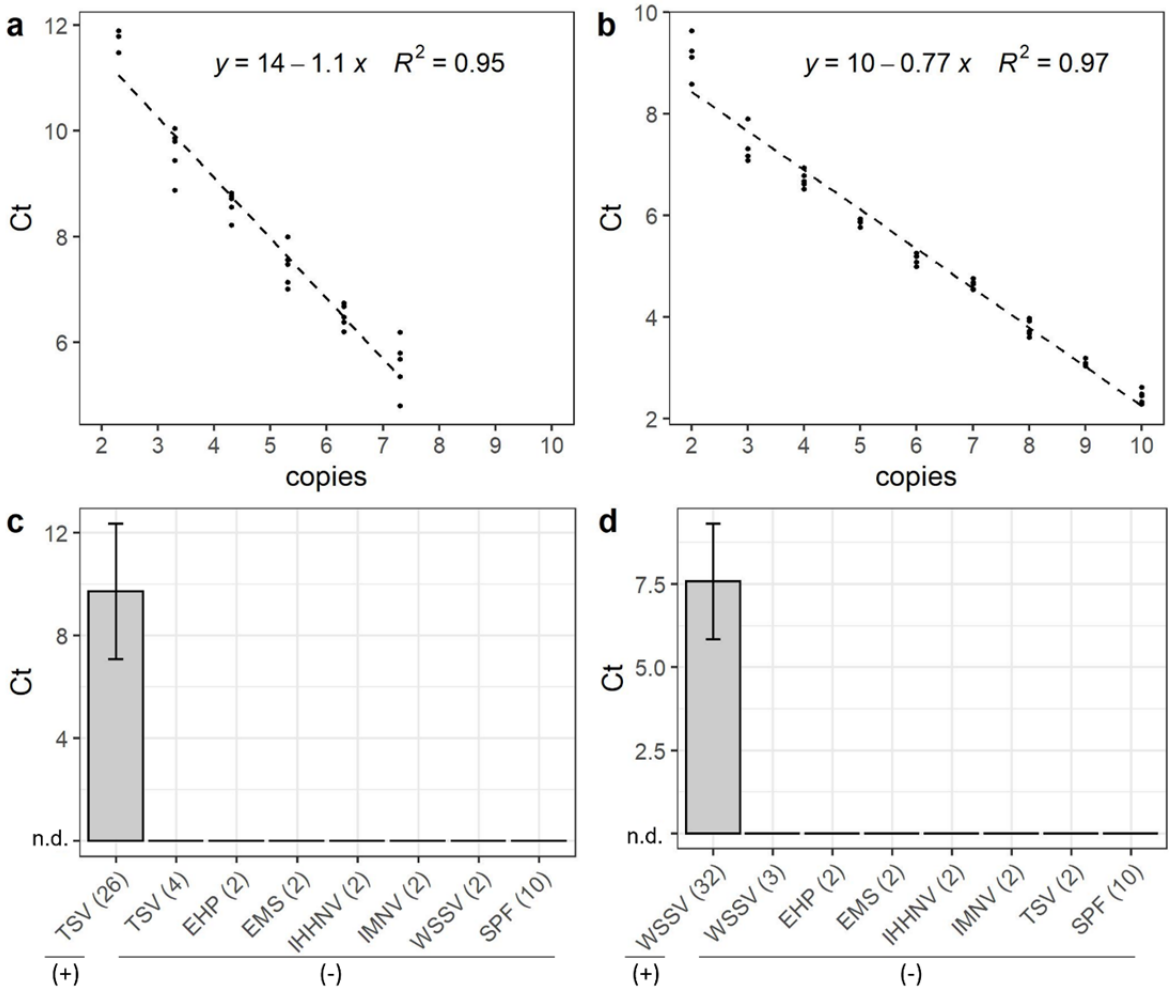

Figure 4. Sensitivity and specificity of SHERLOCK assays. SHERLOCK assay 10-fold standard curve showing Ct values for synthetic (**a**) TSV RNA and (**b**) WSSV DNA target with the dashed line indicating linear regression. Ct values (mean +/- s.d).; n.d., not detected) from SHERLOCK specificity tests evaluating the detection of (**c**) TSV and (**d**) WSSV in shrimp samples known to be infected with TSV, WSSV, and other common white shrimp pathogens including *Vibrio spp.* (causing EMS), EHP, IHHNV, IMNV, and pathogen-free shrimp (SPF). (+) and (-) indicate SHERLOCK results.

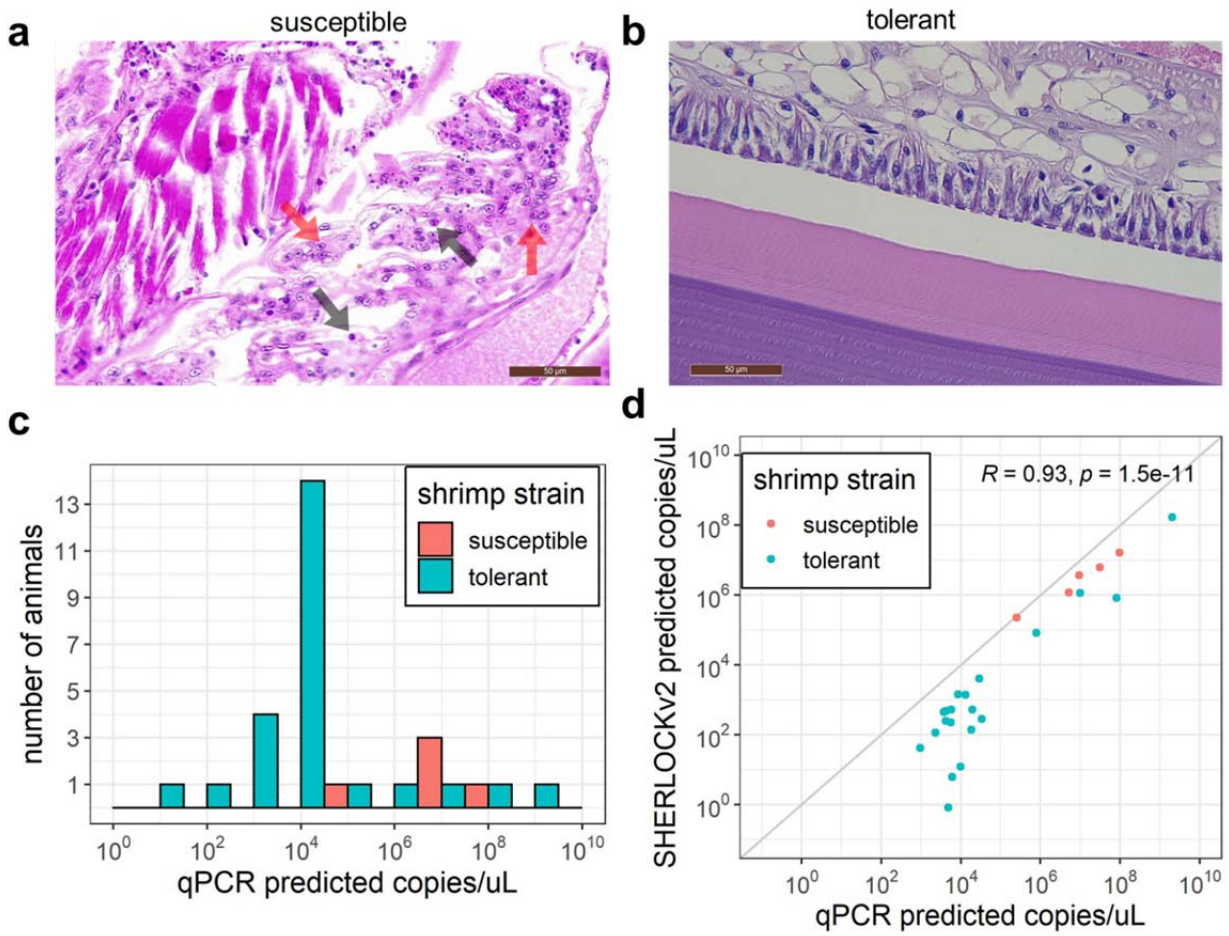

Figure 5. TSV SHERLOCK validation. (**a**) H & E-stained representative section from *P. vannamei* susceptible line after TSV exposure showing focal acute-phase infection in the gill characterized by spherical intracytoplasmic inclusions bodies (black arrows), pyknosis (red arrows) and karyorrhexis. (**b**) H & E-stained representative section from *P. vannamei* resistant line after TSV exposure showing no pathological signs characteristic of TSV infection. (**c**) TSV load quantified by qPCR in resistant (coral) and susceptible animals (teal). (**d**) Correlation between qPCR and TSV SHERLOCK quantification. Gray diagonal line indicates a 1:1 correlation.

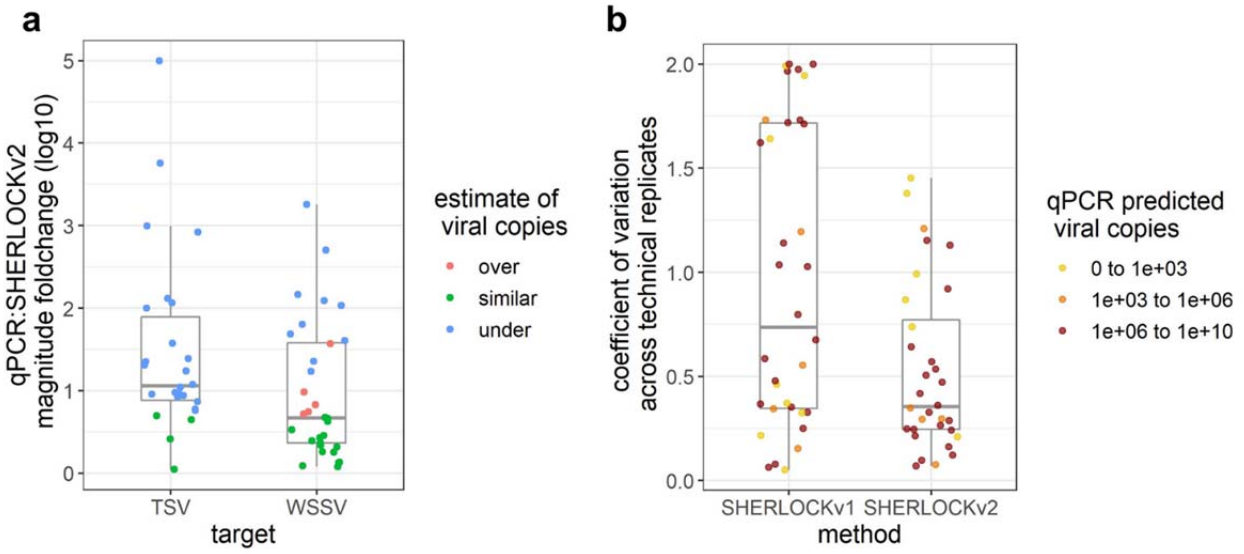

712
713

714 **Figure 6.** Comparison of SHERLOCKv2 assays to existing molecular assays. (**a**) Magnitude fold
715 change in viral copies estimated by SHERLOCKv2 assays relative to qPCR assays for samples
716 tested in both qPCR and SHERLOCK methods. (**b**) Variation across technical replicates for
717 WSSV samples tested in both SHERLOCKv1 and SHERLOCK v2 assays.

718

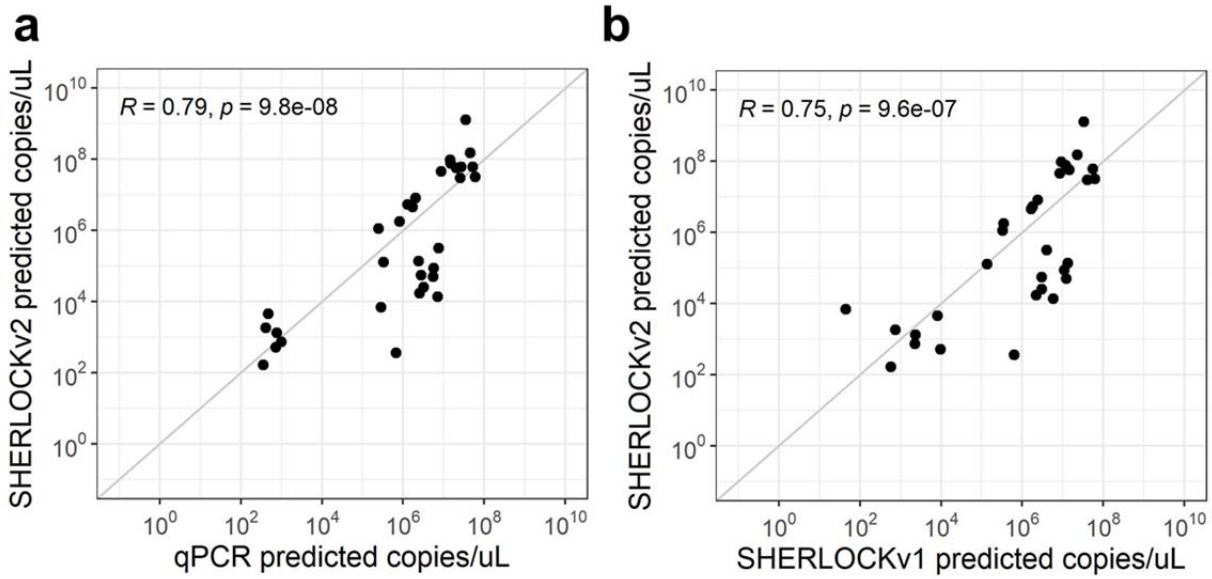

719
720 **Figure 7.** WSSV SHERLOCK assay validation. (**a**) Correlation between qPCR and WSSV

721 SHERLOCKv2 assay quantification. (**b**) Correlation between WSSV SHERLOCKv2 and WSSV

722 SHERLOCKv1 assays. Gray diagonal lines indicate a 1:1 correlation.

723

724

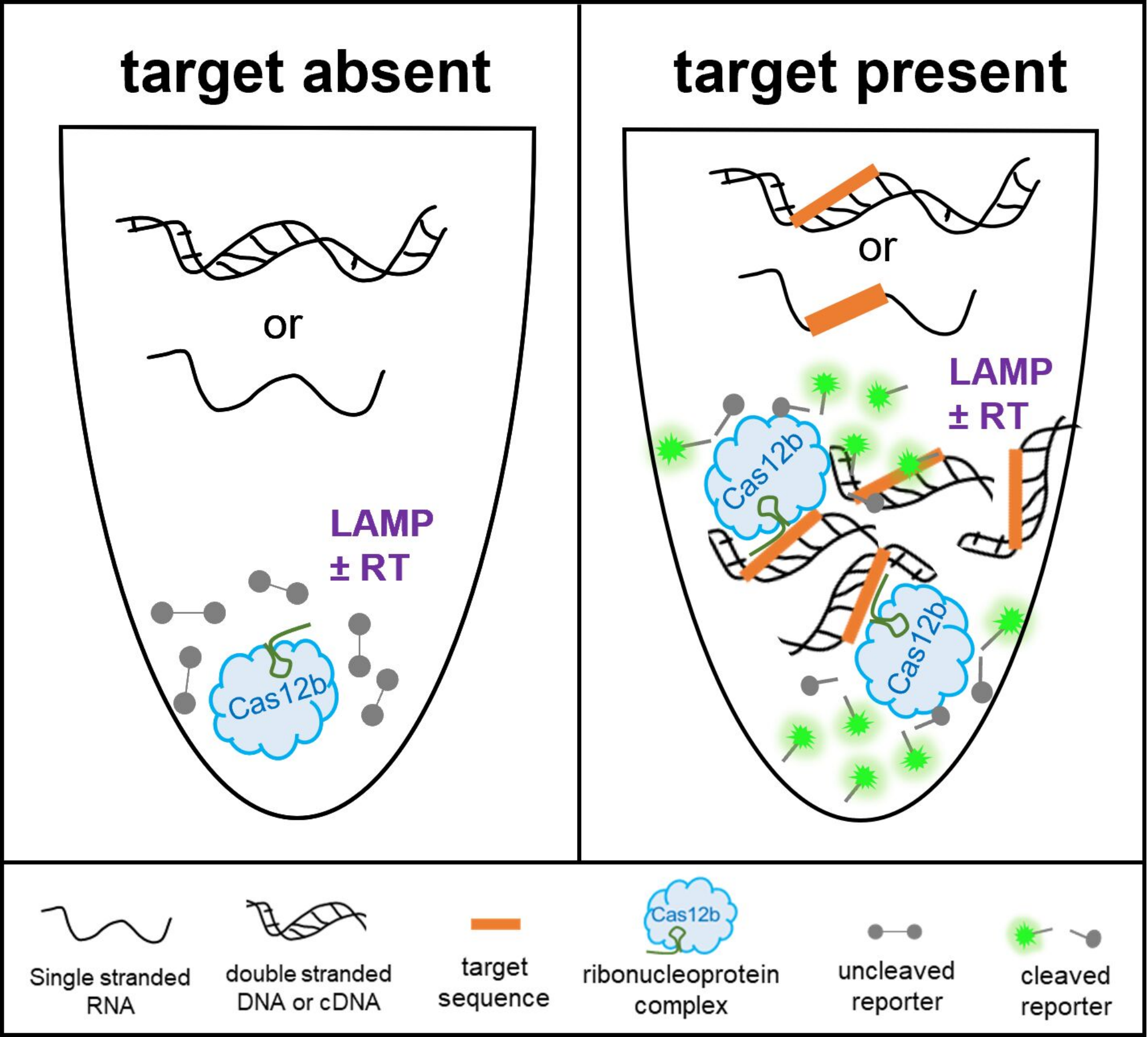
target absent
or
LAMP
± RT
Cas12b
target present
or
LAMP
± RT
Cas12b
Cas12b
Single stranded RNA
double stranded DNA or cDNA
target sequence
Cas12b
ribonucleoprotein complex
uncleaved reporter
cleaved reporter

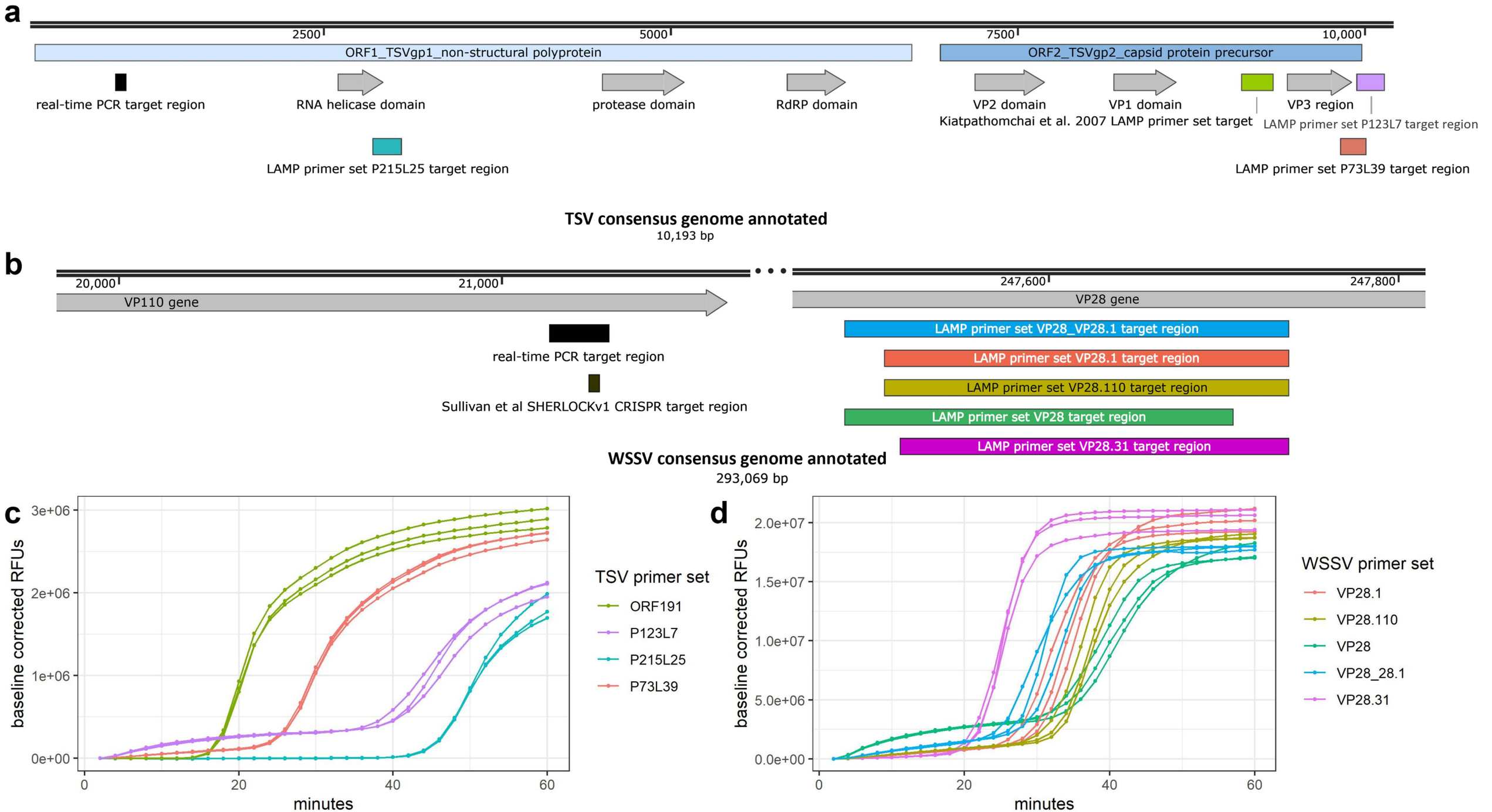
a
2500
5000
7500
10,000
ORF1_TSVgp1_non-structural polyprotein
ORF2_TSVgp2_capsid protein precursor
real-time PCR target region
RNA helicase domain
protease domain
RdRP domain
VP2 domain
VP1 domain
VP3 region
Kiatpathomchai et al. 2007 LAMP primer set target
LAMP primer set P123L7 target region
LAMP primer set P215L25 target region
LAMP primer set P73L39 target region
TSV consensus genome annotated
10,193 bp
b
20,000
21,000
247,600
247,800
VP110 gene
VP28 gene
LAMP primer set VP28_VP28.1 target region
real-time PCR target region
LAMP primer set VP28.1 target region
LAMP primer set VP28.110 target region
Sullivan et al SHERLOCKv1 CRISPR target region
LAMP primer set VP28 target region
LAMP primer set VP28.31 target region
WSSV consensus genome annotated
293,069 bp
c
baseline corrected RFUs
3e+06
2e+06
1e+06
0e+00
0
20
40
60
minutes
TSV primer set
ORF191
P123L7
P215L25
P73L39
d
baseline corrected RFUs
2.0e+07
1.5e+07
1.0e+07
5.0e+06
0.0e+00
0
20
40
60
minutes
WSSV primer set
VP28.1
VP28.110
VP28
VP28_28.1
VP28.31

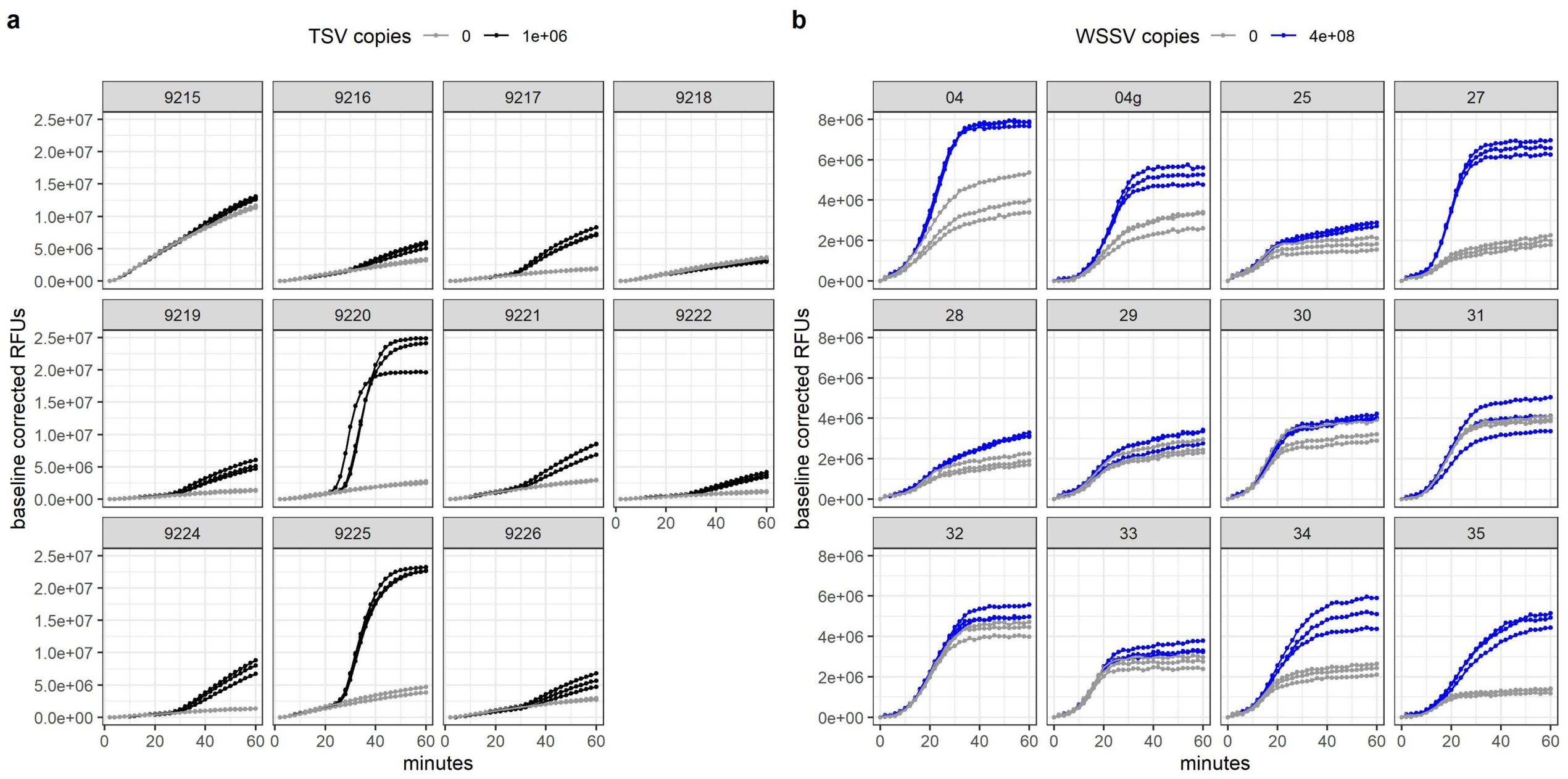
a
TSV copies
0
1e+06
9215
9216
9217
9218
9219
9220
9221
9222
9224
9225
9226
baseline corrected RFUs
minutes
b
WSSV copies
0
4e+08
04
04g
25
27
28
29
30
31
32
33
34
35
baseline corrected RFUs
minutes

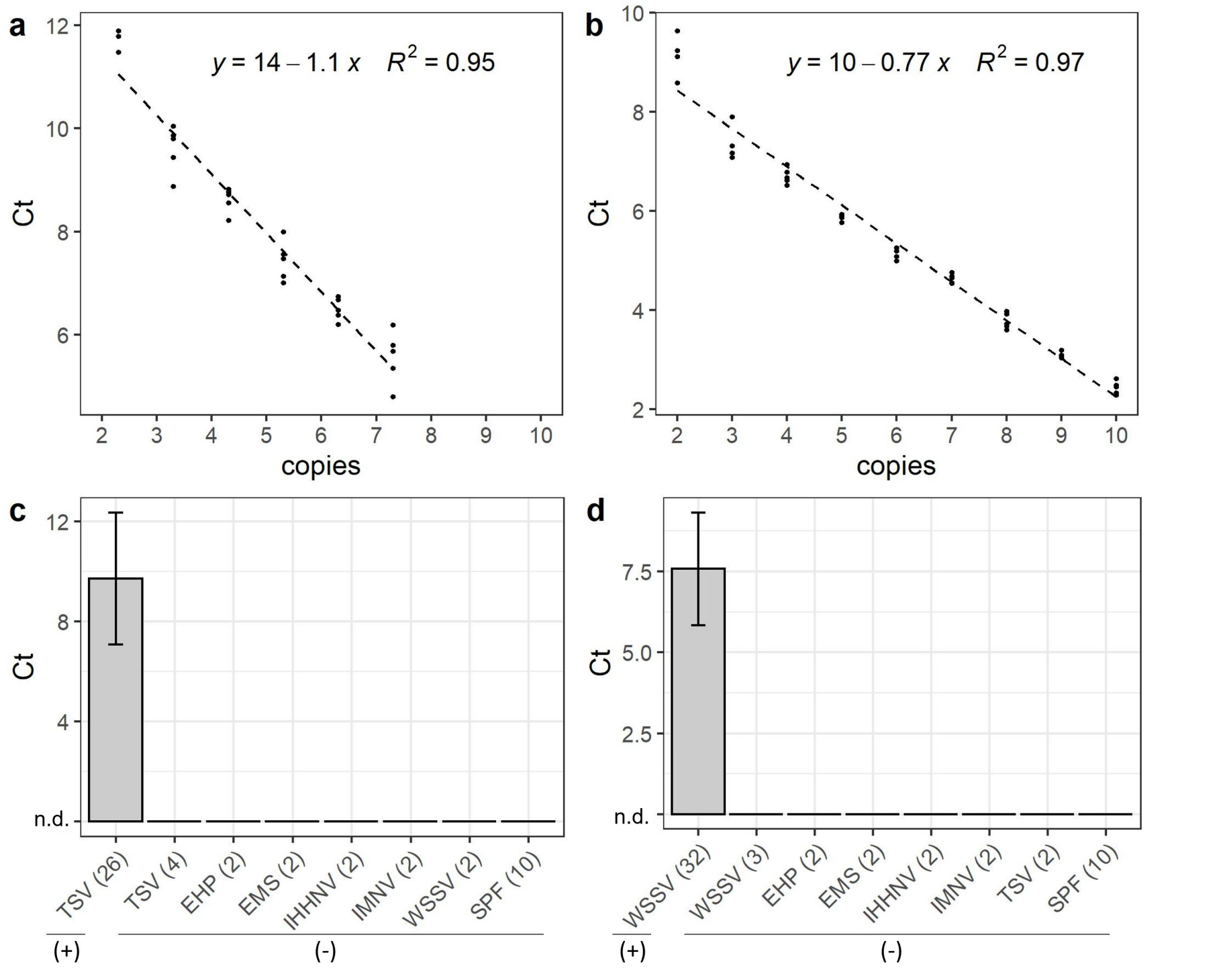
a
y = 14 – 1.1 x R2 = 0.95
Ct
copies
b
y = 10 – 0.77 x R2 = 0.97
Ct
copies
c
Ct
n.d.
TSV (26)
TSV (4)
EHP (2)
EMS (2)
IHHNV (2)
IMNV (2)
WSSV (2)
SPF (10)
(+)
(-)
d
Ct
n.d.
WSSV (32)
WSSV (3)
EHP (2)
EMS (2)
IHHNV (2)
IMNV (2)
TSV (2)
SPF (10)
(+)
(-)

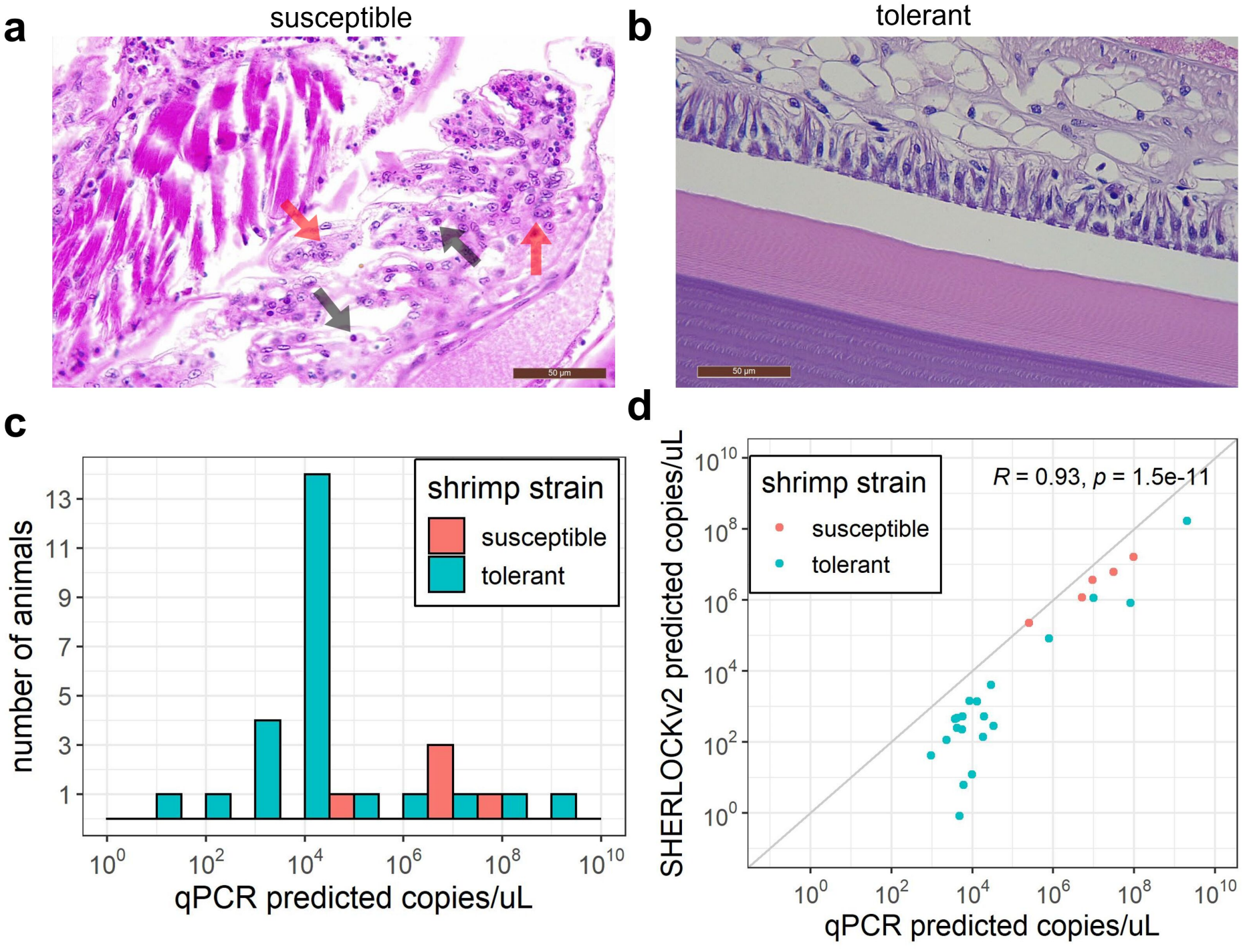
a
susceptible
50 µm
b
tolerant
50 µm
c
shrimp strain
susceptible
tolerant
number of animals
1
3
5
7
9
11
13
10^0
10^2
10^4
10^6
10^8
10^{10}
qPCR predicted copies/uL
d
shrimp strain
susceptible
tolerant
R = 0.93, p = 1.5e-11
SHERLOCKv2 predicted copies/uL
10^0
10^2
10^4
10^6
10^8
10^{10}
qPCR predicted copies/uL

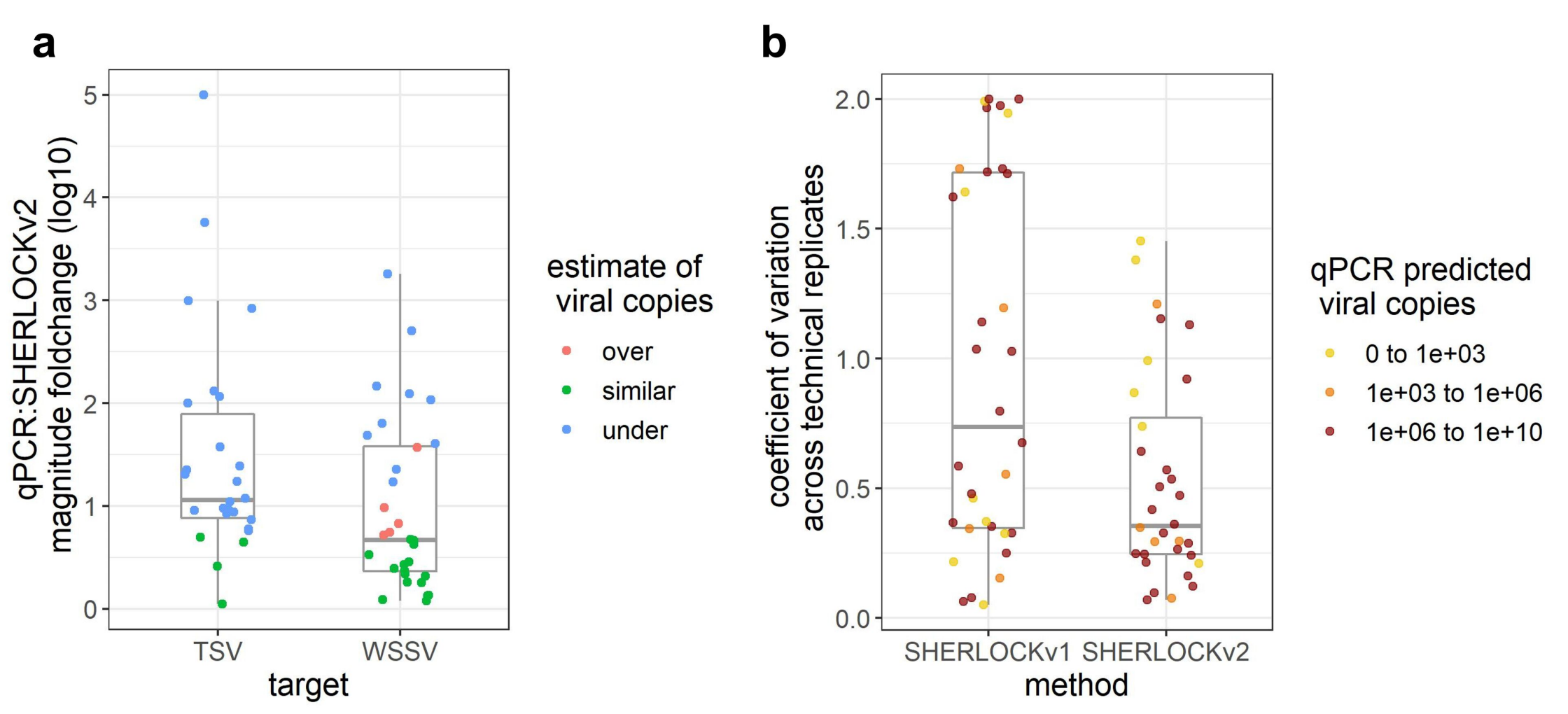
a
qPCR:SHERLOCKv2
magnitude foldchange (log10)
5
4
3
2
1
0
TSV
WSSV
target
estimate of
viral copies
over
similar
under
b
coefficient of variation
across technical replicates
2.0
1.5
1.0
0.5
0.0
SHERLOCKv1
SHERLOCKv2
method
qPCR predicted
viral copies
0 to 1e+03
1e+03 to 1e+06
1e+06 to 1e+10

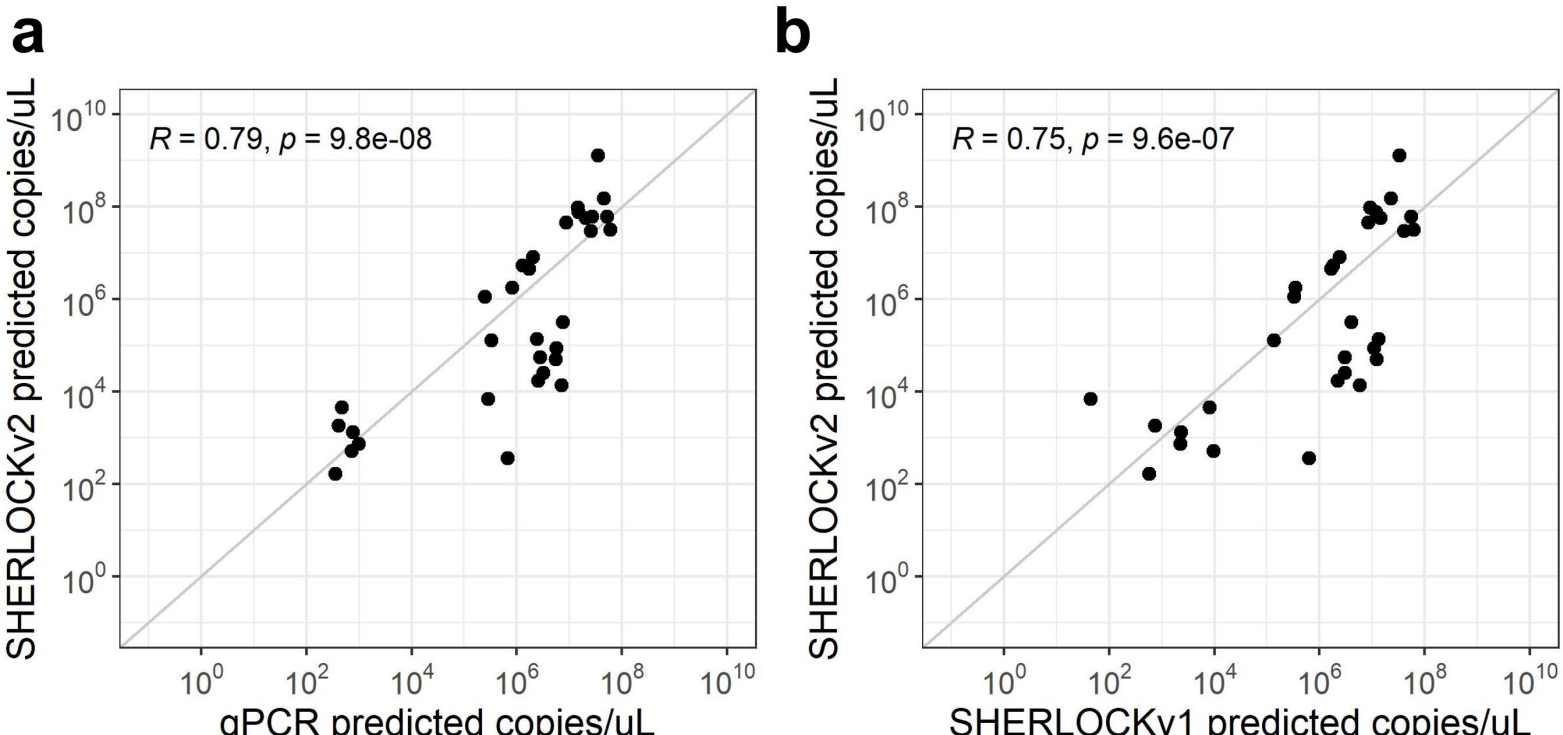
a
R = 0.79, p = 9.8e-08
SHERLOCKv2 predicted copies/uL
qPCR predicted copies/uL
b
R = 0.75, p = 9.6e-07
SHERLOCKv2 predicted copies/uL
SHERLOCKv1 predicted copies/uL